Rit Veðurstofu Íslands

Þóra Árnadóttir
Halldór Geirsson
Bergur H. Bergsson
Christof Völksen

The Icelandic continuous GPS network – ISGPS

March 18, 1999 – February 20, 2000

Þóra Árnadóttir
Halldór Geirsson
Bergur H. Bergsson
Christof Völksen

The Icelandic continuous GPS network – ISGPS

March 18, 1999 – February 20, 2000

CONTENTS

1 SUMMARY

The Icelandic Meteorological Office (IMO) operates a network of continuous Global Positioning System stations in Iceland to monitor crustal deformation. The network is called ISGPS. Four stations are in the Hengill triple junction area and two are south of Mýrdalsjökull. The main purpose of the network is to monitor these two volcanic areas that have shown signs of unrest with increased seismicity in the Hengill area since mid-1994, and Mýrdals- and Eyjafjallajökull since mid-1999. The GPS stations were installed during the period from March to October 1999. Two more stations are planned near Eyjafjallajökull, and one in Vestmannaeyjar, in the year 2000. This report describes the ISGPS network, instrumentation and some technical details, as well as first results of the data processing, as of February 20, 2000. We process the data using the Bernese V4.2 software and calculate daily station coordinates and uncertainties. From the time series of daily station coordinates we estimate east, north and up components of the station velocities. The time series are still short for most of the stations, so these velocity estimates are rather uncertain. The vertical velocity estimate is further downgraded due to large vertical offsets (up to 22 mm) observed when antenna radomes were installed. The largest signal is at station VOGS, which is moving east relative to REYK at about 70% of the expected NUVEL-1A velocity of the North American plate relative to the Eurasian plate. The station at Ölkelduháls shows no significant horizontal motion nor subsidence. The time series at the stations near Mýrdalsjökull are too short, and the displacements too small to allow meaningful velocity estimates for these stations.

2 INTRODUCTION

GPS measurements have been performed to measure crustal deformation in Iceland since 1986 (Foulger et al. 1987). Until now the emphasis has been on network measurements, *e.g.,* Camitz et al. (1995); Foulger (1987); Hackman et al. (1990); Heki et al. (1993); Jahn (1990); Sigmundsson et al. (1993); Sturkell et al. (1994); Sigmundsson et al. (1995); Hreinsdóttir et al. (2000). Network measurements allow good spatial coverage, but rather poor resolution of temporal variation in deformation rates. A number of large continuous GPS (CGPS) networks have been initiated during the last 5 years, the largest to date is in Japan with over a thousand stations. Several volcanic centers are monitored with CGPS, for example Kilauea volcano on Hawaii (Lisowski et al. 1996) and Long Valley Caldera in east central California (Dixon et al. 1997). The advantage of using CGPS in regions where deformation can be complex both spatially and temporally, is that frequent measurements can be made with high precision. If the sites are carefully chosen, a few stations (depending on the complexity of the system) can give accurate information on the strain accumulation of the area over a period spanning from hours to years. The drawback of CGPS is that the instruments are still rather expensive, and it is not yet possible to monitor the deformation in real-time with sub-centimeter precision, in the same way as, for example, continuous volumetric strain measurements can be used (Linde et al. 1993). High precision GPS measurements require use of precise orbits that are not available until about 2 weeks after the measurements. Data processing of short sessions, less than 24 hours, also degrades the precision. Several research groups are working towards real-time processing of GPS data, which is particularly useful for volcanic hazard monitoring (Hamburger et al. 1999).

The first CGPS station in Iceland was installed in Reykjavík (REYK) on November 2, 1995, by a German group at Bundesamt für Kartographie und Geodäsie (BKG, formerly IFAG). The station is located on the roof of a building at the University of Iceland, and is a part of the International GPS Service (IGS) network. The same group installed a GPS/GLONASS station,

REYZ, next to REYK on September 11, 1998. Data from REYZ are not publically available at present. The second CGPS station in Iceland was installed by the German group in Höfn, Hornafjörður (HOFN) on May 27, 1997. This station is a part of the European Reference Frame (EUREF) network (EUREF 2000). The Icelandic Maritime Administration (IMA) operates 6 coastal stations for differential GPS. These stations are L1 only, and located on top of lighthouses. In addition IMA has a dual frequency station at its central office in Kópavogur, where the antenna is on a 15 m high mast.

3 THE ISGPS NETWORK

Seismic activity at the Hengill triple junction in SW Iceland increased in mid-1994. Figure 1 shows a map of the Hengill area. Besides horizontal shearing, the earthquakes have been linked to continuing uplift in the Hrómundartindur area, at a rate of about 2 cm/yr since 1993 (Sigmundsson et al. 1997; Feigl et al. 2000). The largest earthquake sequence to date started on June 3, 1998, culminating in a M_L=5.1 earthquake on June 4, followed by an unusually long period of aftershocks, that lasted for over two weeks (Ágústsson 1998; Árnadóttir et al. 1999). A second earthquake sequence started on November 13, 1998, with a M_L=5.0 earthquake in the Ölfus area, and an aftershock sequence that lasted 3 days (Rögnvaldsson et al. 1998b). These earthquake sequences and measurements of continuous uplift caused public concern and funding to purchase four GPS instruments to use for continuous measurements was obtained from the Icelandic Government and the Reykjavík District Heating (now Reykjavík Energy). The first continuous GPS station in the ISGPS network was installed at Vogsósar (VOGS) and started collecting data on March 18, 1999. The antenna is placed a few meters from the SIL seismic station VOS (Rögnvaldsson et al. 1998a). The station in Hveragerði (HVER) started on March 25, 1999, Hlíðardalsskóli (HLID) on May 21, 1999, and Ölkelduháls (OLKE) on May 25, 1999 (see Figure 1 for the station locations).

In July 1999 seismicity increased at Mýrdals- and Eyjafjallajökull, which are two subglacial volcanic centers in South Iceland. Figure 2 shows a map of the Mýrdalsjökull area. A small jökulhlaup occurred in Jökulsá á Sólheimasandi, which flows southwest from Mýrdalsjökull, on July 18, 1999 (Einarsson 2000). Katla volcano is located beneath Mýrdalsjökull, and the latest large eruption was in 1918. Eyjafjallajökull last erupted in 1821–1823. These volcanoes are near populated areas, and their eruptions can generate large jökulhlaups and ash plumes.

Two continuous GPS stations have been installed to monitor these volcanoes, and two more are planned in the year 2000. Funding for three GPS instruments was obtained from the Icelandic Research Council (RANNÍS) in 1999, to use for network and semi-continuous measurements. The station on Sólheimaheiði (SOHO) was installed on September 24, 1999, and a second station at Láguhvolar (HVOL) became operational on October 19, 1999 (see Figure 2).

The Department of Geophysics at the Icelandic Meteorological Office (IMO) operates a system of 37 digital seismometers (the SIL system) (Stefánsson et al. 1993; Böðvarsson et al. 1996). In view of the monitoring responsibility of the IMO it was decided that IMO would install, operate and analyze data from the CGPS network in Iceland. The new network is called ISGPS and is shown in Figure 3. Table 1 lists the station information. The plan was originally to co-locate the CGPS stations with SIL seismic stations to minimize operation cost of the network. Each SIL station is equipped with a PC computer running the UNIX operating system, and is connected to the IMO through an X.25 link (Böðvarsson et al. 1999). Few of the SIL stations are ideally located for monitoring crustal deformation at volcanic centers in Iceland. It was
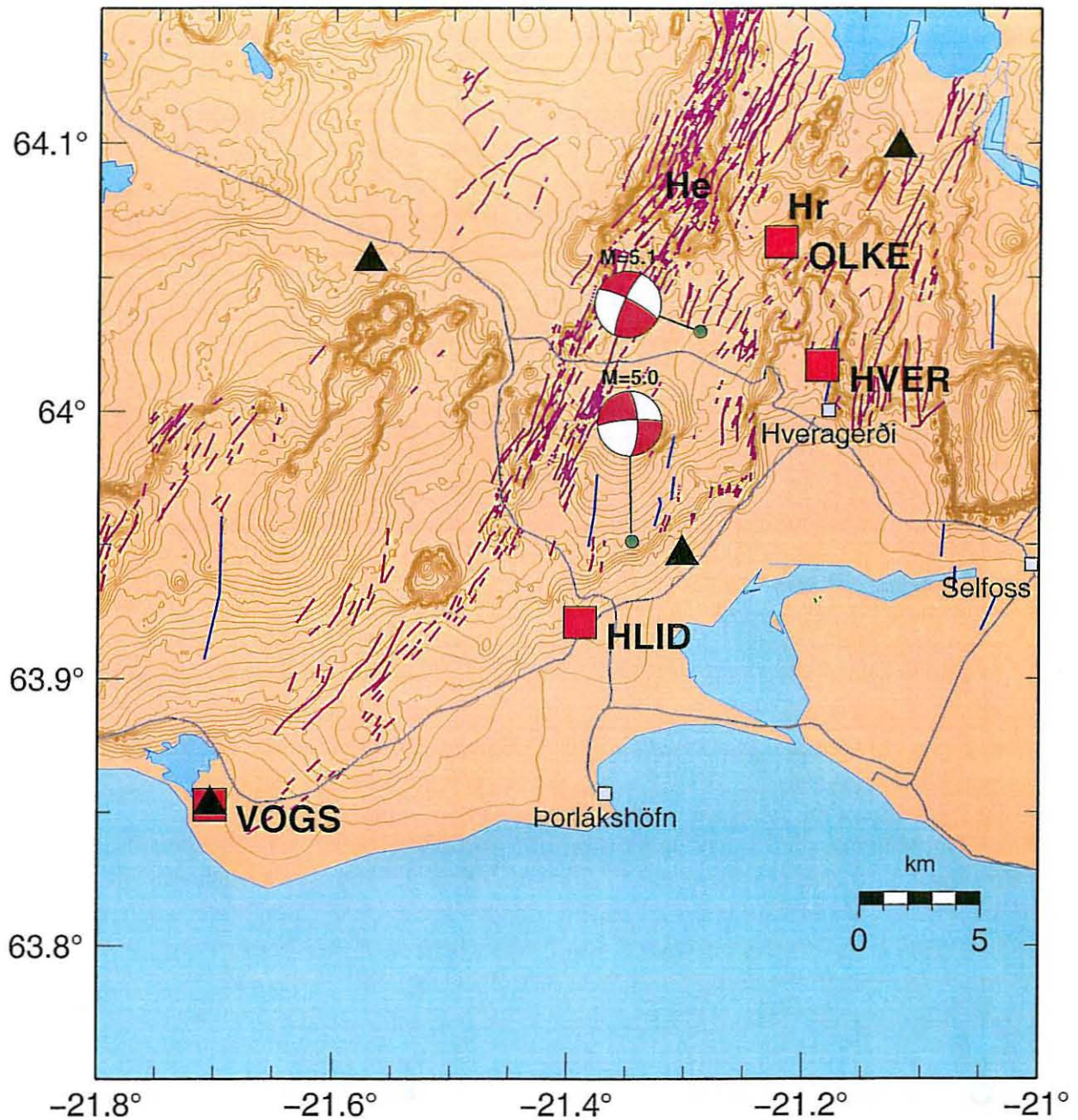
Figure 1. *Map of the Hengill triple junction in SW Iceland.* Hr *is Hrómundartindur and* He *is Hengill. Black triangles are SIL seismic stations. Red squares are the ISGPS stations. Station OLKE is near Ölkelduháls. The epicentral locations of the* M_L=5.1 *June 1998 and the* M_L=5.0 *November 1998 earthquakes are shown with green dots as well as their focal mechanisms. Roads are shown with gray lines. Mapped normal faults and fissures are shown with purple lines and N-S trending strike-slip faults with blue lines (Sæmundsson 1995; Erlendsson 1996).*
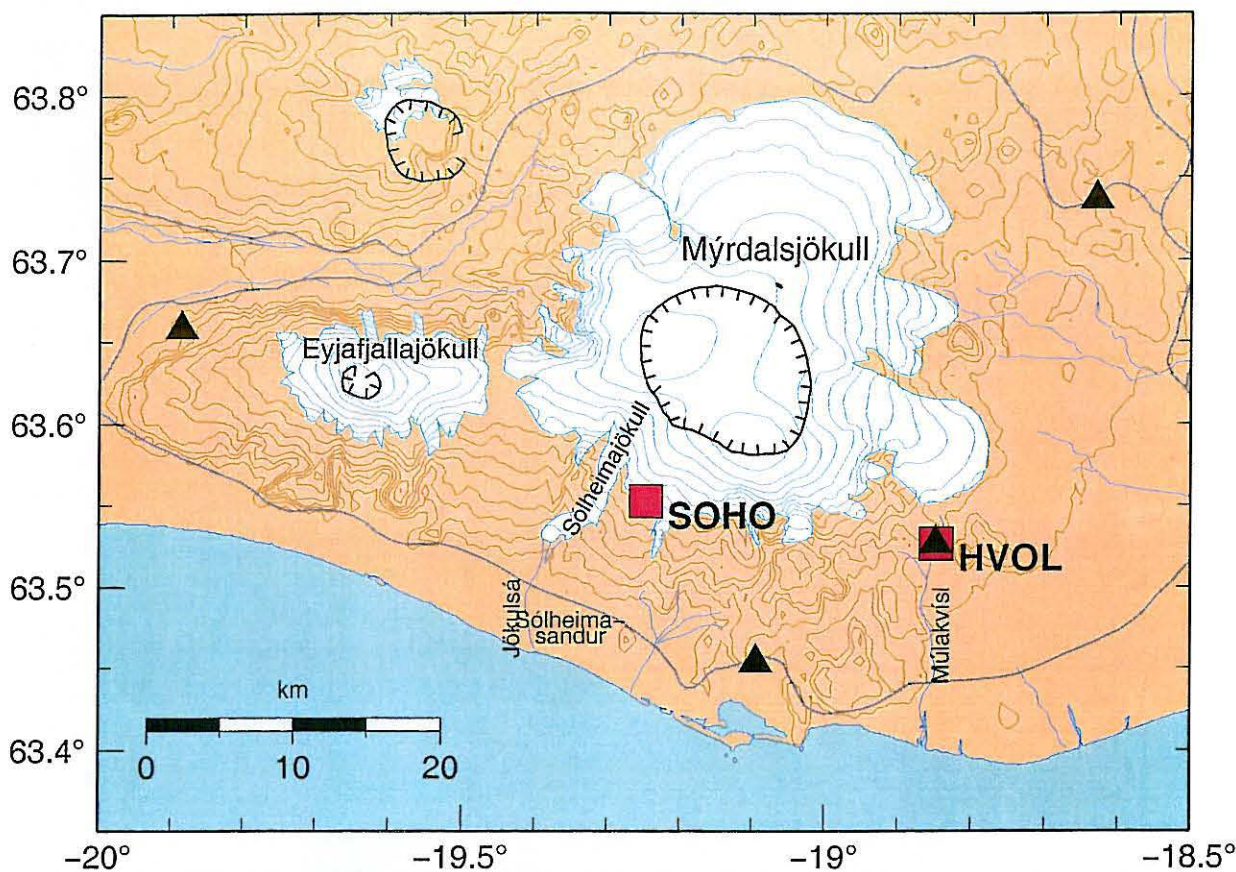
Figure 2. *Map of Mýrdals- and Eyjafjallajökull. Red squares are continuous GPS stations, and black triangles are SIL seismic stations. The calderas of Katla and Eyjafjallajökull are shown on the figure as black lines with tick marks.*

Station	Lat. (°N)	Lon. (°W)	Elevation (m)	Receiver	Antenna height (m)
HLID	63.92110	21.38970	45.5	Trimble 4700	0.9089
HVER	64.01715	21.18481	84.4	Trimble 4700	0.9843
HVOL	63.52628	18.84754	199.3	Trimble 4000SSI	1.0443
OLKE	64.06312	21.21989	484.9	Trimble 4700	0.9742
SOHO	63.55247	19.24665	791.6	Trimble 4000SSI	1.0121
VOGS	63.85269	21.70365	7.6	Trimble 4700	0.9721
REYK	64.13878	21.95548	27.6	Rouge SNR-8000	0.0680

Table 1. *List of stations, coordinates, elevation above sea level, instrument type and vertical antenna heights to the antenna ground plane. The station elevation measured by GPS is height above the reference ellipsoid. The height above sea level is calculated by subtracting the geoid height from the ellipsoidal height. The geoid height we used was obtained from the National Land Survey of Iceland.*
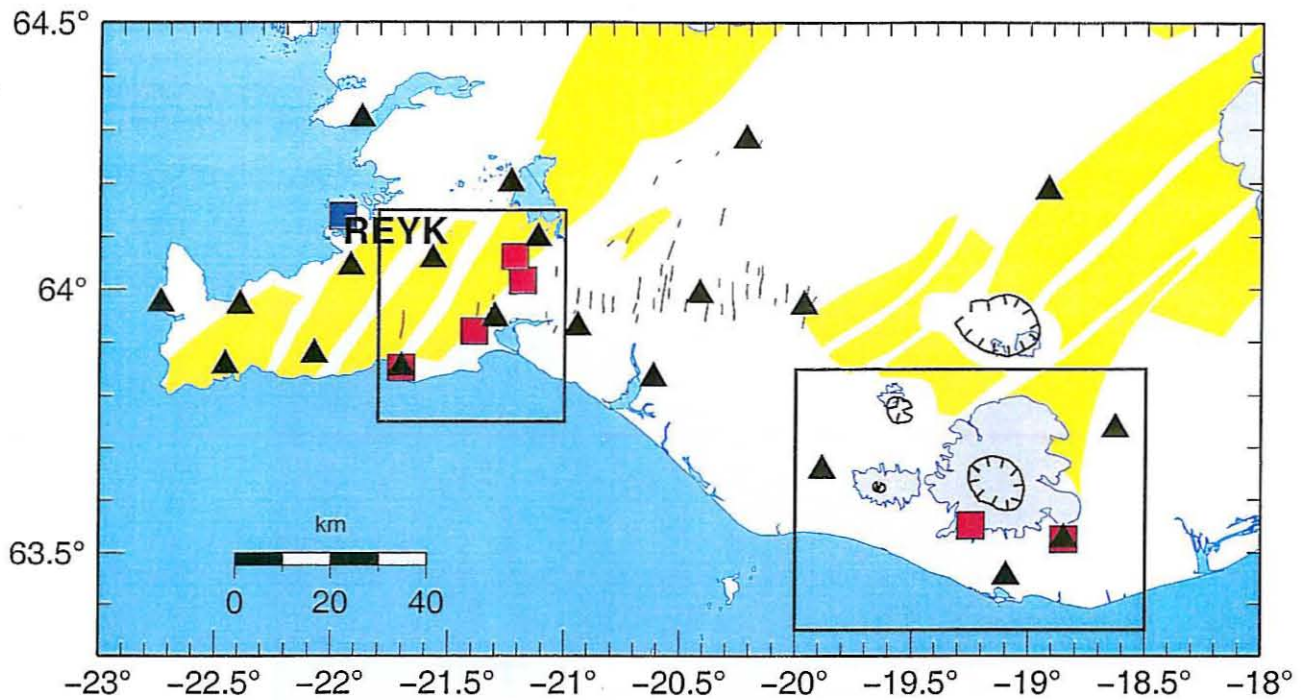
8

Figure 3. *Map of southwest part of Iceland showing the location of the continuous GPS stations in the ISGPS network (red squares), the continuous GPS station REYK (blue square) and SIL seismic stations (black triangles). The black boxes show locations of the detailed maps (Figures 1 and 2). The yellow areas are volcanic fissure swarms, and the calderas are shown with black lines with tick marks. Thin black lines denote mapped faults (Einarsson and Sæmundsson 1987; Erlendsson 1996).*

therefore decided to install some of the CGPS stations at optimal locations for detecting volcanic deformation, despite more costly operation than if they were co-located with SIL stations.

The ISGPS network uses Trimble 4700 and Trimble 4000SSI GPS instruments and Trimble choke ring antennas. Both types of receivers are dual-frequency systems, *i.e.,* track both L_1 and L_2 signals. They are capable of tracking up to 12 satellites simultaneously and record both P-code and carrier phase data at 15 s intervals. Each antenna is mounted on a one meter high stainless steel quadripod that is bolted and cemented into stable bedrock. A geodetic monument (pin) is also installed to make it possible to replace the antennas with high accuracy. Figure 4 shows the instrument installation at station HVOL. Gray plastic domes (radomes) from the Southern California Integrated GPS Network (SCIGN) are used to protect the antennas from snow, ice and possible vandalism.

At present there is no software available for UNIX or LINUX that can facilitate remote downloading of data from the Trimble 4700 receivers. We use the *Universal Reference Station* (URS) software from Trimble to control the Trimble 4700 instruments, collect the raw data and transform the data into RINEX format (Gurtner 1994). The URS software runs on a PC under the Windows operating system. The data are remotely downloaded via modem once every 24 hours from the IMO. Figure 5 shows a schematic diagram of the instrument setup at station HVER.

The setup at the stations running Trimble 4000SSI receivers is somewhat different. The data are collected into the internal memory of the receivers and the UNAVCO software Lapdogs (UNAVCO 1999) is used to remotely download the raw data to the IMO once every 24 hours. The data are then translated into RINEX format at the IMO using the Bernese software TR-
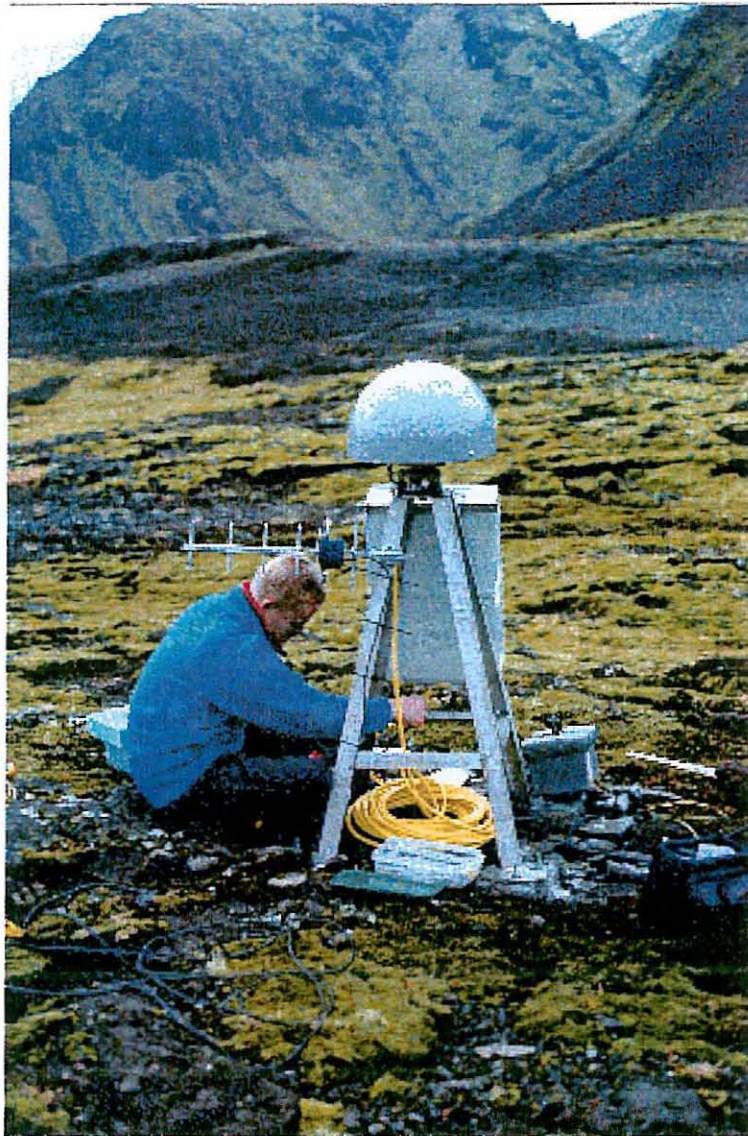
Figure 4. *Installation of a GPS instrument at station HVOL. The antenna is mounted on a stainless steel quadripod, and an antenna radome (gray plastic) covers the antenna. The receiver is in a box on the side of the quadripod. The data are collected from the receiver via cellular telephone once every 24 hours.*
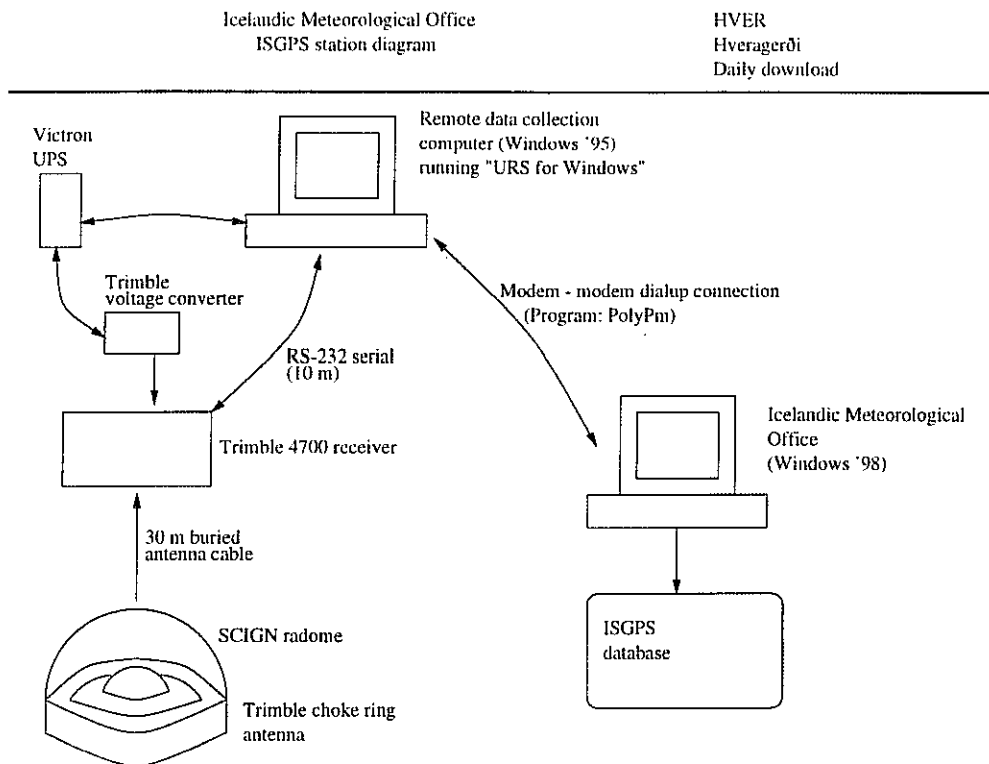
Icelandic Meteorological Office
ISGPS station diagram

HVER
Hveragerði
Daily download

Victron
UPS

Remote data collection
computer (Windows '95)
running "URS for Windows"

Trimble
voltage converter

Modem - modem dialup connection
(Program: PolyPm)

RS-232 serial
(10 m)

Trimble 4700 receiver

Icelandic Meteorological
Office
(Windows '98)

30 m buried
antenna cable

SCIGN radome

ISGPS
database

Trimble choke ring
antenna

Figure 5. *Schematic diagram of station setup. The receiver is operated by a PC computer and the URS software by Trimble. The receiver gathers data from the antenna and sends them to the PC. The URS software does not allow the data to be stored in the memory of the receiver. The raw data are translated into RINEX format and stored in a folder on the PC. Once every 24 hours the RINEX files are collected from the PC by the IMO via a modem.*
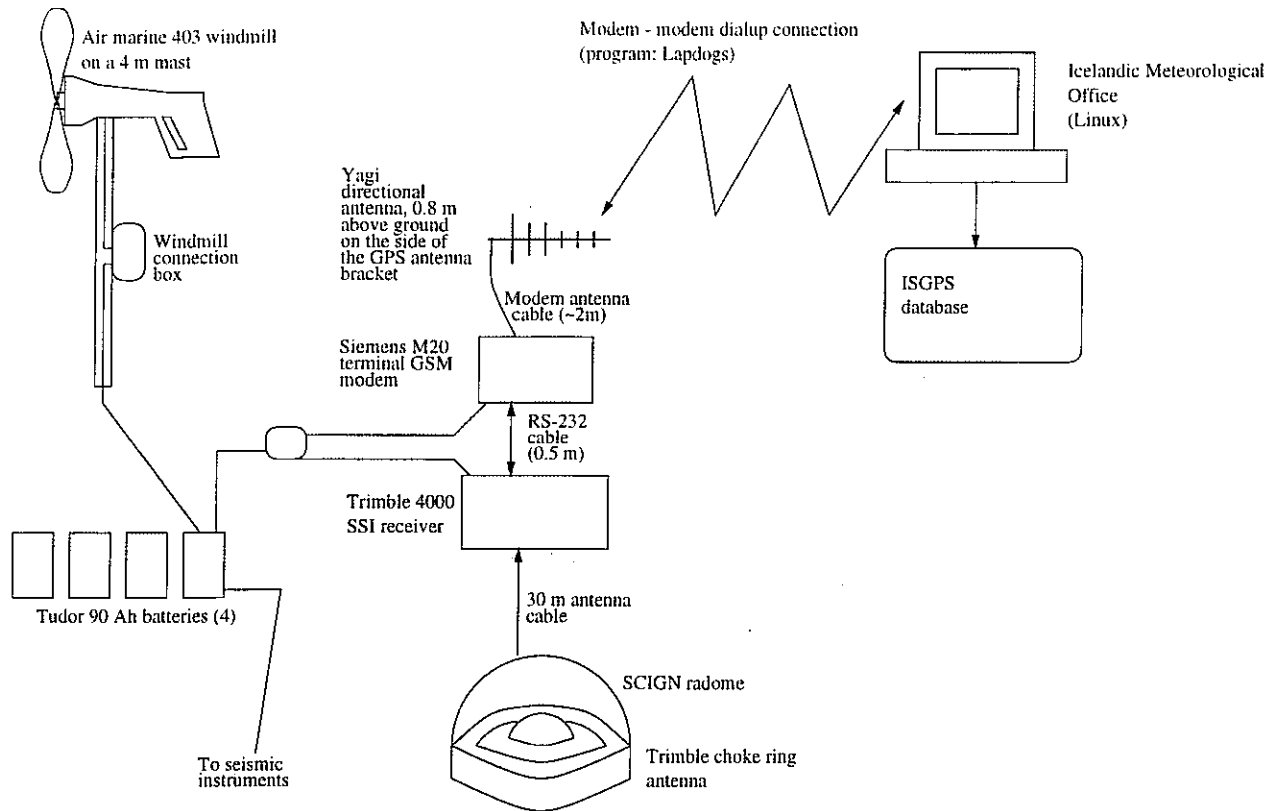
Figure 6. *Schematic diagram of station setup at HVOL with a Trimble 4000SSI instrument. The satellite signals are received by the antenna and transformed into data and stored in the internal memory of the receiver. Once every 24 hours the raw data files are collected directly from the receiver by the IMO via a modem.*

RINEXO (before March 2, 2000) and the UNAVCO software TEQC (UNAVCO 1999; Estey and Meertens 1999). Figure 6 shows a schematic diagram of the station setup at HVOL.

The data are available to the general public via the internet a few hours after they are retrieved from the stations (just after midnight GMT). The URL is: *http://www.vedur.is/ja/gps.html*. We use data from the International GPS Service (IGS) station in Reykjavík (REYK) as a reference station for our network. The station REYK has a Rouge SNR-8000 receiver and a Dorne Margolin choke ring antenna, and is located on the roof of a building at the University of Iceland. The data from REYK (24 hour RINEX files) are available via anonymous ftp from *igs.ifag.de* a few hours after the measurements are performed.

4 DATA PROCESSING

We will not describe the technical details of the GPS system in this report, but refer interested readers to *e.g.*, Leick (1990) and Rothacher and Mervart (1996). When the data have been downloaded to the IMO they are processed using the Bernese V4.0 and V4.2 (after January 1, 2000) software (Rothacher and Mervart 1996). We use precise orbits from the Center for Orbit Determination in Europe (CODE) which are available by anonymous ftp from *ubeclu.unibe.ch*,

about 2 weeks after the measurements. The CODE orbits are in the International Terrestrial Reference Frame 1997 (ITRF97) (Boucher et al. 1999), as of August 1, 1999 (T. Springer, pers. communication, 1999). The satellites also broadcast orbits which are in the World Geodetic System 1984 (WGS-84) reference frame. These orbits are rarely used as they are less precise than CODE orbits. The uncertainty in the CODE final orbits is reported as 0.05 m whereas the uncertainty of the broadcast orbits is 3 m. An orbital error of 2.5 m causes an error of 0.1 ppm in baseline estimation, whereas an orbital error of 0.05 m causes 0.002 ppm error in baseline. For real-time GPS analysis it is better to use CODE predicted orbits, which have a reported error of 0.2 m, than the broadcast orbits (Rothacher and Mervart 1996). We use data from the International GPS Service (IGS) station in Reykjavik (REYK) in our analysis. Data from REYK are used in the CODE orbit determination, hence our ISGPS network coordinates are in the ITRF97 reference frame. We use ITRF97 epoch 1997.0 station coordinates and velocities to update the coordinates for REYK each week.

We follow the same processing strategy as used for the European network solution (Rothacher and Mervart 1996). This is a different strategy than used in processing GPS measurements from network campaigns by the Nordic Volcanological Institute (Hreinsdóttir 1999). The main difference is that we use the geometry-free (L_4) linear combination rather than the wide-lane (L_5) combination (see discussion below). We estimate station coordinates using 24 hours of data and a constant 15° elevation angle cut-off, *i.e.*, data from satellites that are less than 15° above the horizon are not included in the analysis. The first several steps follow the routine processing scheme of the Bernese software. The orbits are converted into the correct format using the program PRETAB and one standard arc orbit for each day generated with ORBGEN. The RINEX data files are translated into Bernese format with the program RXOBV3. Then three preprocessing programs are used. First, CODSPP computes the receiver clock error and estimates station coordinates using zero difference code measurements. In the next step, SNGDIF creates the phase single difference files between receivers from observations at the same time. Finally, MAUPRP computes the triple difference residual for all the observations, corrects big jumps that usually originate from receiver clocks, and deletes cycle slips.

Now the actual parameter estimation program GPSEST is run to calculate precise station coordinates. This program is run several times to obtain the final solution. In the first run the program estimates station coordinates using the ionosphere-free linear combination (L_3), where the ionospheric path delay is practically eliminated (Rothacher and Mervart 1996). We use the Saastamoinen model to correct for the signal delay due to the troposphere at each site (Rothacher and Mervart 1996). The improved station coordinates are then used in the next run of GPSEST where we constrain all the station coordinates and estimate an ionospheric model using the geometry-free linear combination (L_4) which is independent of receiver clocks and geometry (*i.e.*, orbits and station coordinates). It contains the ionospheric delay and the initial phase ambiguities (Rothacher and Mervart 1996). GPSEST is run for the third time using the ionospheric model estimated in the previous step. In this run we constrain the coordinates of REYK, and estimate and save the L_1 and L_2 ambiguities. In the final run of GPSEST the L_1 and L_2 ambiguities are introduced, and the L_3 linear combination used to calculate the final station coordinates.

In the final step of GPSEST we calculate the final station coordinates and full covariance matrix for the daily solutions. Systematic errors or mismodelled parameters are not included in the formal error estimate done by GPSEST. Therefore the uncertainty in the final station coordinates reported by GPSEST is underestimated. A more accurate estimate of the error can

13

be obtained by calculating the average station coordinates for each week using the Bernese network adjustment program COMPAR (Rothacher and Mervart 1996). COMPAR calculates a network solution from a given set of daily solutions and the variation of the daily solutions from the network solution. The variation gives a more realistic estimate of the error in the daily coordinate solutions than the formal uncertainty calculated by GPSEST. We find that the errors in the station coordinates estimated by GPSEST should be scaled by a factor of 3 to obtain an improved error estimate. Figure 7 shows histograms for the difference between weekly network solutions and the daily solutions, after removing outliers (see below). The RMS repeatability in the daily coordinates for the stations is about 3 mm in north and east, but about 11 mm in vertical. The large uncertainty in the vertical component is due to the satellite geometry (all the signals from satellites come from above ground) and the variable troposphere and ionosphere delays of the signal that are difficult to estimate accurately.

5 RESULTS

To monitor crustal deformation measured by the ISGPS network we calculate the station motions relative to REYK in east, north and up, relative to the station coordinates at a reference epoch. For example, we calculate the average station coordinates for GPS week 1012 (May 30 – June 5, 1999) using COMPAR. We then use these average station coordinates as a reference for the Hengill area, since all the stations there were in operation by this time. The station displacements are then calculated relative to the average station coordinates during GPS week 1012, assuming that REYK does not move. From the displacement time series we can calculate the station velocities for each component (east, north and up) by fitting a straight line to the station displacements and their uncertainties (*i.e.,* calculate the weighted linear least squares solution). The weighted residual sum squared is,

$$WRSS = r^T \Sigma^{-1} r, \tag{1}$$

where r is the residual vector, *i.e.,* the difference between the observed and predicted data, and Σ is the data covariance matrix. In this case we do not consider correlated errors, so Σ is a diagonal matrix. The number of degrees of freedom for the problem is $\nu = N - m$ where N is the number of data and m is the number of unknowns. When fitting a straight line to the data, *i.e.,* solving $F(t) = at + b$, where t is time and $F(t)$ is the displacement, we have two unknowns, a and b. To test how well the data are fit by the straight line model we can calculate the value $\chi^2_\nu = WRSS/\nu$. A $\chi^2_\nu = 1.0$ indicates that the model is a good fit to the data and the error estimates of the data are appropriate. Before the data can be modelled we need to remove outliers from the datasets, as they can have a large effect on the model in a linear least squares problem such as this one. Outliers are identified as days with large difference between the daily solution and a weekly network solution, calculated with COMPAR. If the difference is larger than 20 mm in north or east component or 45 mm in vertical, we remove all components of data for that day from the analysis. Data with uncertainties larger than 5 times the RMS values for each coordinate are also removed.

Table 2 lists the calculated station velocities and uncertainties at the 2σ level, assuming a constant rate for each component of motion. We find that there are large offsets (up to 22 mm) in the vertical component, that appear to be caused by the antenna radome installation. We estimate the vertical velocity before and after radome installation where the time series are long enough to yield meaningful estimates. Apparent offsets in east and north due to radome installation are not easily detectable for these time series. We are currently testing the effect of radome installa-
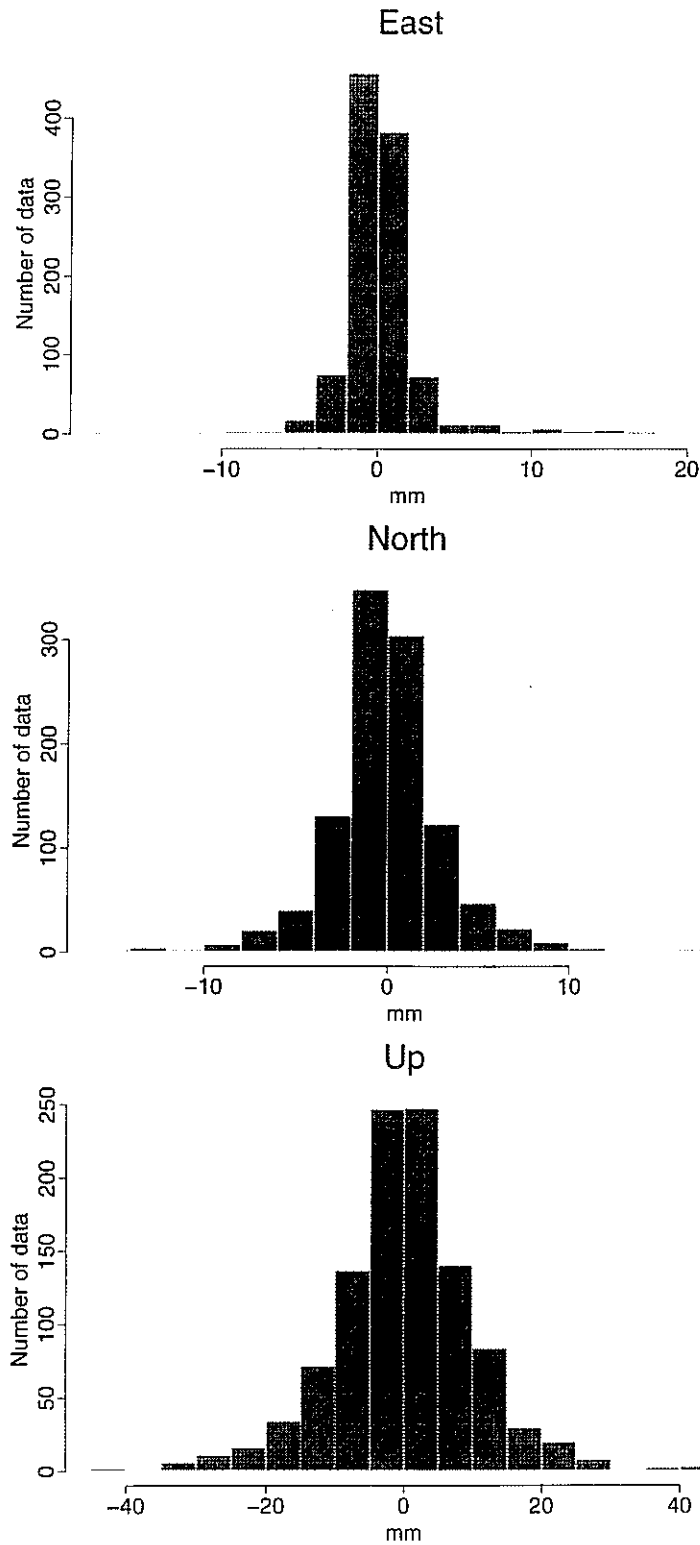
14

Figure 7. *Histograms showing the variation of daily solutions relative to a weekly network solution calculated by COMPAR, in east, north and up coordinate in millimeters. The scatter in the daily solutions are normally distributed with mean zero for all components.*

15

Station	N	V_E (mm/yr)	V_N (mm/yr)	V_{U1} (mm/yr)	V_{U2} (mm/yr)
HLID	166	9 ± 2	-2 ± 3	28 ± 23	30 ± 27
HVER	267	4 ± 1	-5 ± 1		
HVOL	63	3 ± 8	5 ± 10		-48 ± 30
OLKE	202	1 ± 1	2 ± 2		0 ± 5
SOHO	78	10 ± 4	5 ± 6		-5 ± 36
VOGS	263	12 ± 1	-2 ± 1	1 ± 8	0 ± 13

Table 2. *Calculated velocities of stations in east, north and up, relative to REYK. N is the number of data, for each component, used in the calculation, V is the velocity, and E, N and U subscripts denote east, north and up respectively. The vertical velocity is estimated before and after radome installation, V_{U1}, and V_{U2} respectively, where possible. The reported uncertainty is at the 2σ level. The velocities are calculated assuming a linear fit to each component of motion during the whole period. Outliers are removed (see discussion in text).*

tion. Tests conducted by the USGS, Scripps, and Jet Propulsion Laboratory (JPL) indicate that the radome introduces less than 0.2 mm changes in horizontal phase center and less than 2 mm changes in vertical phase center (SCIGN 1999).

We limit our analysis to data collected before February 20, 2000, which is day number 51, and the beginning of GPS week 1050. The results are discussed in the following sections.

5.1 The Hengill area

5.1.1 VOGS

Figure 8 shows the horizontal and vertical motion of VOGS relative to REYK as a function of time, and the estimated 1σ uncertainty of each measurement. We have estimated the velocity of VOGS relative to REYK by fitting a straight line through each component of the calculated displacements (see discussion above) after removing 12 outliers (days 90, 120, 182, 243, 244, 271, 289, 311, 320, 323, 393 and 403). The best fit line gives rates of motion towards east of about 12 ± 1 mm/yr and $\chi^2_\nu = 1.7$. The velocity in the south direction is 2 ± 1 mm/yr, with $\chi^2_\nu = 1.5$ for the estimate. VOGS appears to be uplifting at a rate of 1 ± 8 mm/yr ($\chi^2_\nu = 0.7$), before day 328, and a rate of 0 ± 13 mm/yr after that ($\chi^2_\nu = 0.7$). The installation of the radome appears to cause a 20 mm vertical offset in the time series. The change in the estimated velocity before and after radome installation is insignificant. A longer time series, without changes in the radome, will yield a better estimate of the long-term vertical rate. The best fit lines are shown as heavy black lines on Figure 8. The east and north components of velocity translate to a motion of 12.2 ± 1 mm/yr in direction N99°E ±1°. The NUVEL-1A plate motion of the Eurasian plate relative to the North American plate is 18.5 mm/yr in direction N103°E (DeMets et al. 1990, 1994). If we assume that VOGS is on the Eurasian plate and REYK is on the North American plate, VOGS appears to be moving at about 70% of the full NUVEL-1A plate velocity relative to REYK.

5.1.2 HVER

We calculate the velocity of HVER relative to REYK for the period shown in Figure 9. We delete 17 outliers (days 182, 201, 244, 270, 283, 311, 315, 317, 320, 322, 323, 325, 337, 346,
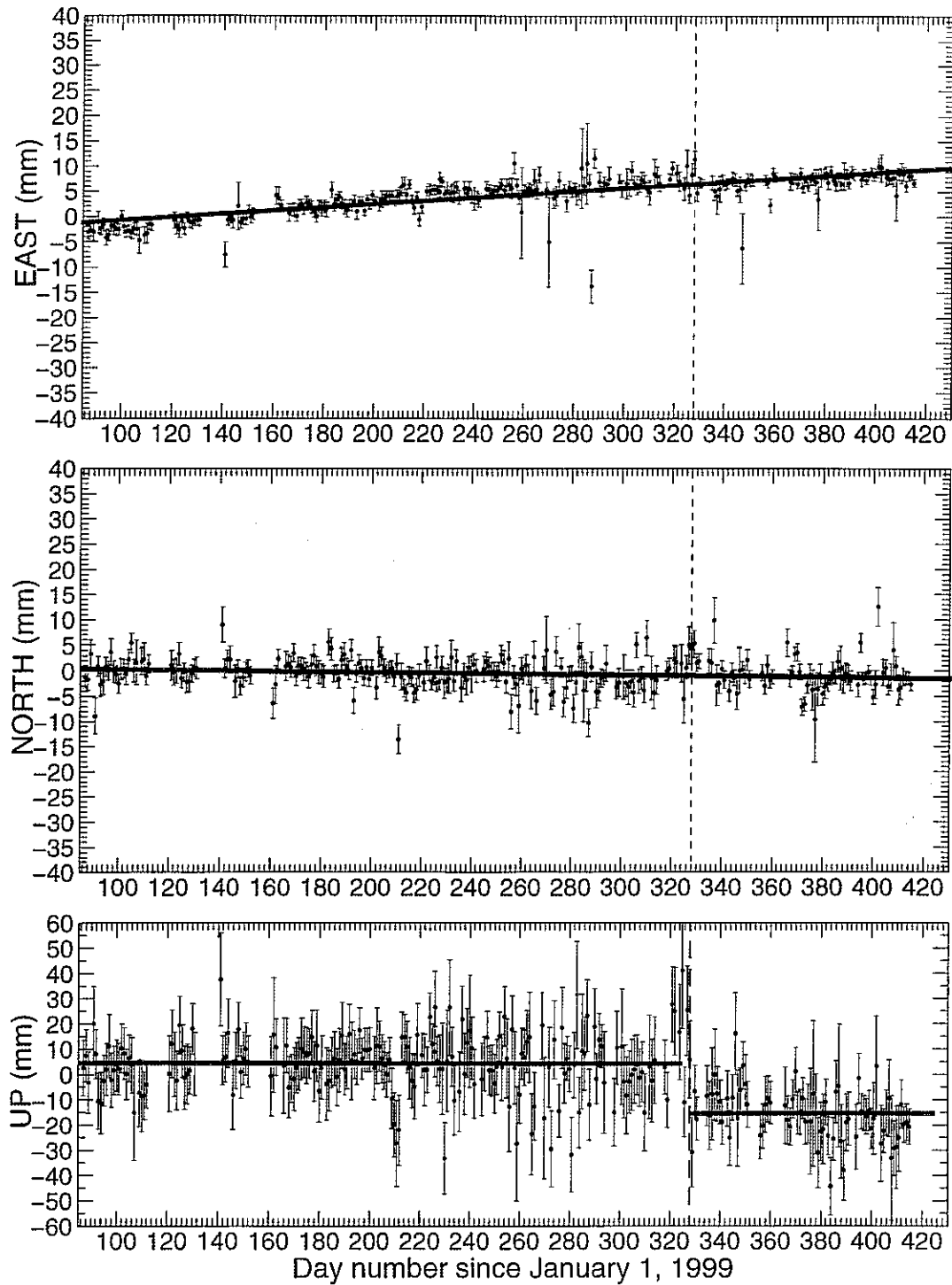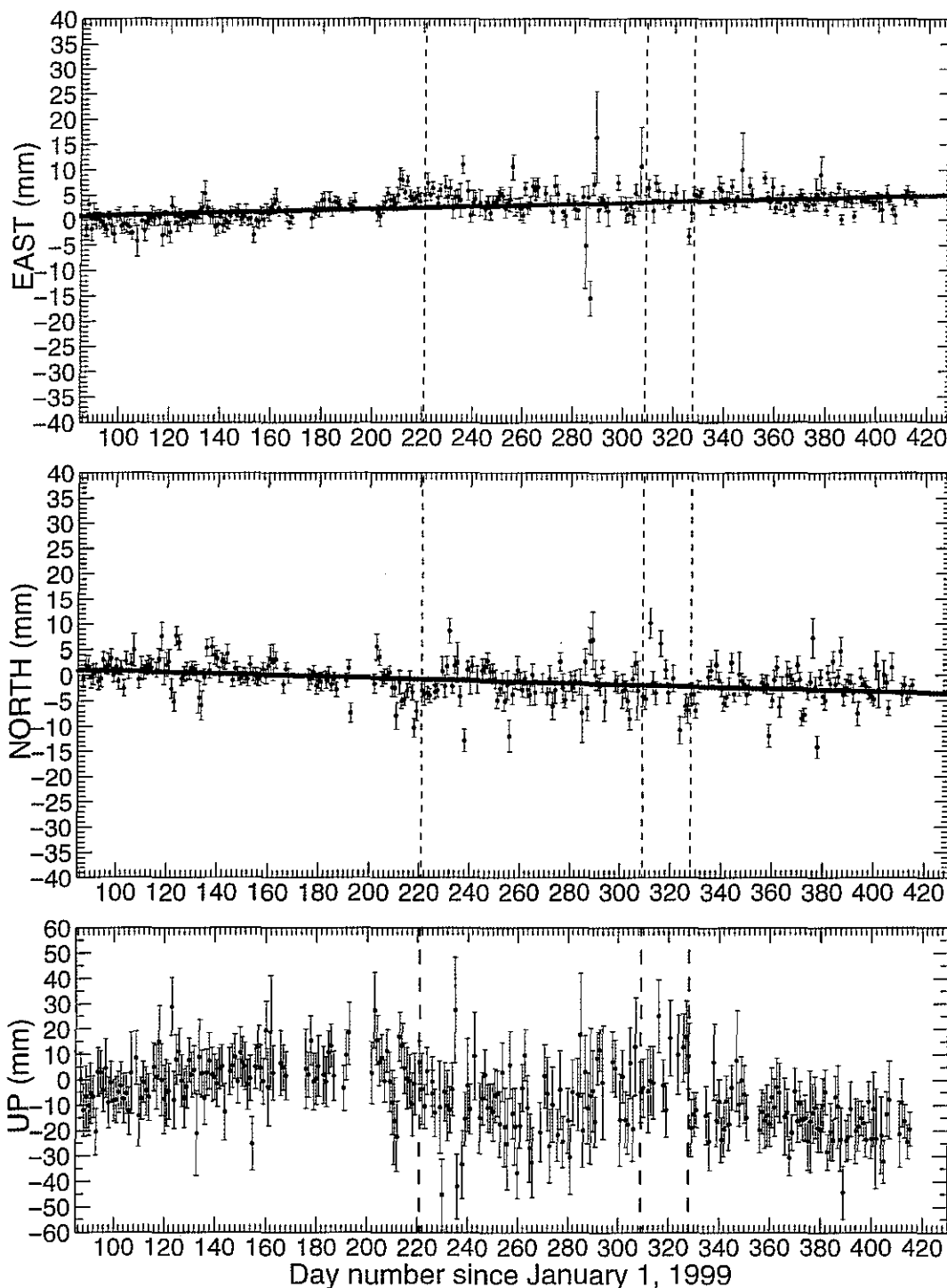
VOGS – REYK

Figure 8. *The horizontal and vertical motion of VOGS relative to REYK as a function of time, since the start of the measurements there. Each dot represents a 24 hour solution. The motion in east, north and up directions is defined to be positive, and is given in units of millimeters. The error bars indicate 1σ confidence limits. The thick black lines show the best fit (weighted least squares) velocities calculated for each component of motion, after outliers have been removed. The antenna radome was installed on day 328 (shown with dotted vertical black lines) causing an estimated 21 mm vertical offset.*

17

HVER – REYK

Figure 9. *The horizontal and vertical motion of HVER relative to REYK as a function of time, since the start of the measurements there. Each dot represents a 24 hour solution. The motion in east, north and up directions is defined to be positive, and is given in units of millimeters. The error bars indicate 1σ confidence limits. The thick black lines show the best fit (weighted least squares) velocities calculated for each component of motion, after outliers have been deleted. The antenna radome was first installed on day 221, taken off on day 309 and installed again on day 328 (shown with dotted vertical black lines). The radome was re-oriented on day 235. We do not estimate the vertical velocity because the time series are too short between changes in the radome.*

18

393, 403 and 408). Assuming that each component of motion can be fit by a single straight line gives a velocity of 4 ± 1 mm/yr towards east ($\chi^2_\nu = 2.0$) and 5 ± 1 mm/yr southward motion ($\chi^2_\nu = 2.6$). We do not estimate the vertical component of motion because the time series are too short between changes in the radome. There appear to be short period temporal variations in the vertical signal. It is possible that they are due to atmospheric or ionospheric effects that we are not modelling, or local changes influenced by the geothermal system in Hveragerði.

5.1.3 HLID

Figure 10 shows the relative motion of HLID as a function of time. We have estimated the velocity of HLID relative to REYK using data before day 342, 1999. Data after day 341 is not reliable because the antenna at HLID was covered in snow several times after that date. We deleted 19 outliers (days 175, 182, 235, 236, 237, 244, 256, 275, 285, 287, 290, 291, 296, 300, 311, 314, 320, 323, and 325). The best fit line gives velocities of 9 ± 2 mm/yr towards east ($\chi^2_\nu = 1.5$) and 2 ± 3 mm/yr towards south ($\chi^2_\nu = 2.5$). We estimate the vertical velocity before and after radome installation (day 235). Before day 235 the vertical rate of uplift is 28 ± 23 mm/yr ($\chi^2_\nu = 0.7$) and 30 ± 27 mm/yr ($\chi^2_\nu = 0.8$) after day 235. These rates are similar, but barely significant at the 2σ level. We estimate a vertical shift of about 22 mm on day 235, when the antenna radome was installed. This is the largest effect of radome installation we observe in our network.

The effect of snow covering the antenna is apparent as spurious north, east and vertical motion after day 341, 1999, on Figure 10. It is interesting to note that the effect of snow is visible in all the components, not just the vertical. This may be caused by asymmetry in the snow cover over the antenna. Data from the GPS station CASA in Long Valley, that was temporarily covered with snow, showed only vertical changes (Webb et al. 1995). They report a snow thickness of 1–2 m before loss of signal, causing up to almost 40 cm apparent positive vertical motion. On January 14, 2000, we find a positive vertical motion of 21 cm, and 2 cm in eastward and 4 cm southward apparent motion due to snow cover. No measurements of snow thickness or estimates of the geometry of the snow pile were made at HLID. The data from HLID should not be used after day 341, and will not be distributed on the web. The measurements at this station have been discontinued (as of day number 75, 2000) and the antenna will be moved to a better location.

5.1.4 OLKE

Figure 11 shows the relative motion of OLKE in east, north and up as a function of time. Data gaps are due to power failures at OLKE which is a remote station powered by a windmill. Data is continually sent to a computer located on Háhryggur, about 7 km NW of the station. Some loss of data, causing short sessions from days 240–325, 1999, was due to partial blocking of the data transmitter antenna (spread spectrum modem) relative to Háhryggur.

We estimate the velocity of OLKE relative to REYK by fitting a straight line to the individual components of motion. First we delete 23 outliers (days 182, 235, 236, 240, 243, 252, 255, 257, 275, 277, 285, 287, 311, 312, 314, 315, 317, 320, 323, 325, 403, 408 and 410). The velocity we estimate in east direction is 1 ± 1 mm/yr ($\chi^2_\nu = 2.5$), 2 ± 2 mm/yr in north ($\chi^2_\nu = 3.5$) and a vertical rate of 0 ± 5 mm/yr ($\chi^2_\nu = 1.0$) after day 182, when the antenna radome was installed. The time series before day 182 was too short to allow a meaningful estimate of the vertical velocity.
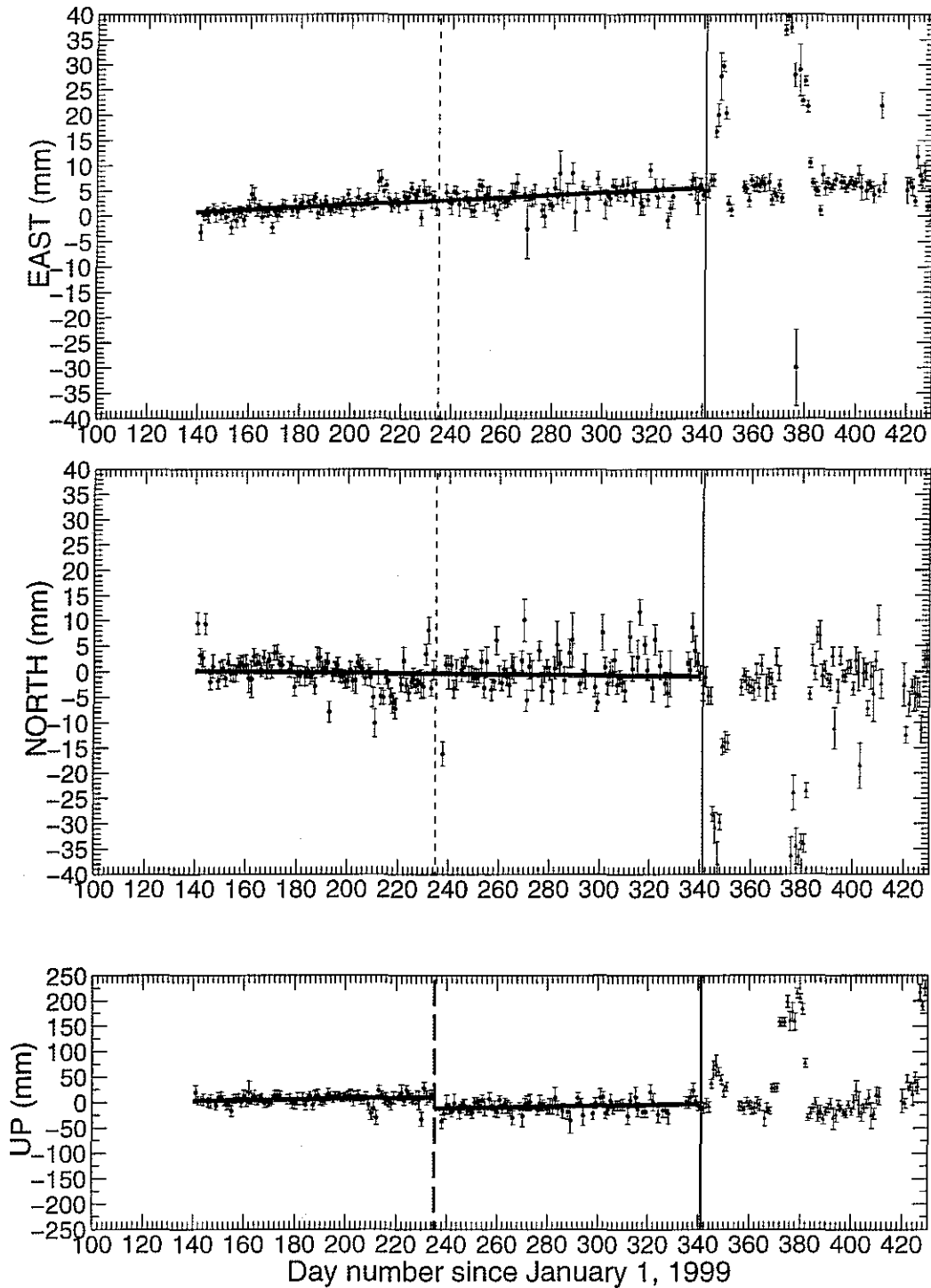
Figure 10. *The horizontal and vertical motion of HLID relative to REYK as a function of time, since the start of the measurements there. Each dot represents a 24 hour solution. The motion in east, north and up directions is defined to be positive, and is given in units of millimeters. The error bars indicate 1σ confidence limits. The thick black lines show the best fit (weighted least squares) velocities calculated for each component of motion, after outliers have been removed. The antenna radome was installed on day 235 (shown with dotted vertical black lines). The antenna was covered with snow several times after day 341 (solid vertical line). The data after that date are not used in the velocity estimation. Note that the scale on the vertical plot is different from other similar figures.*
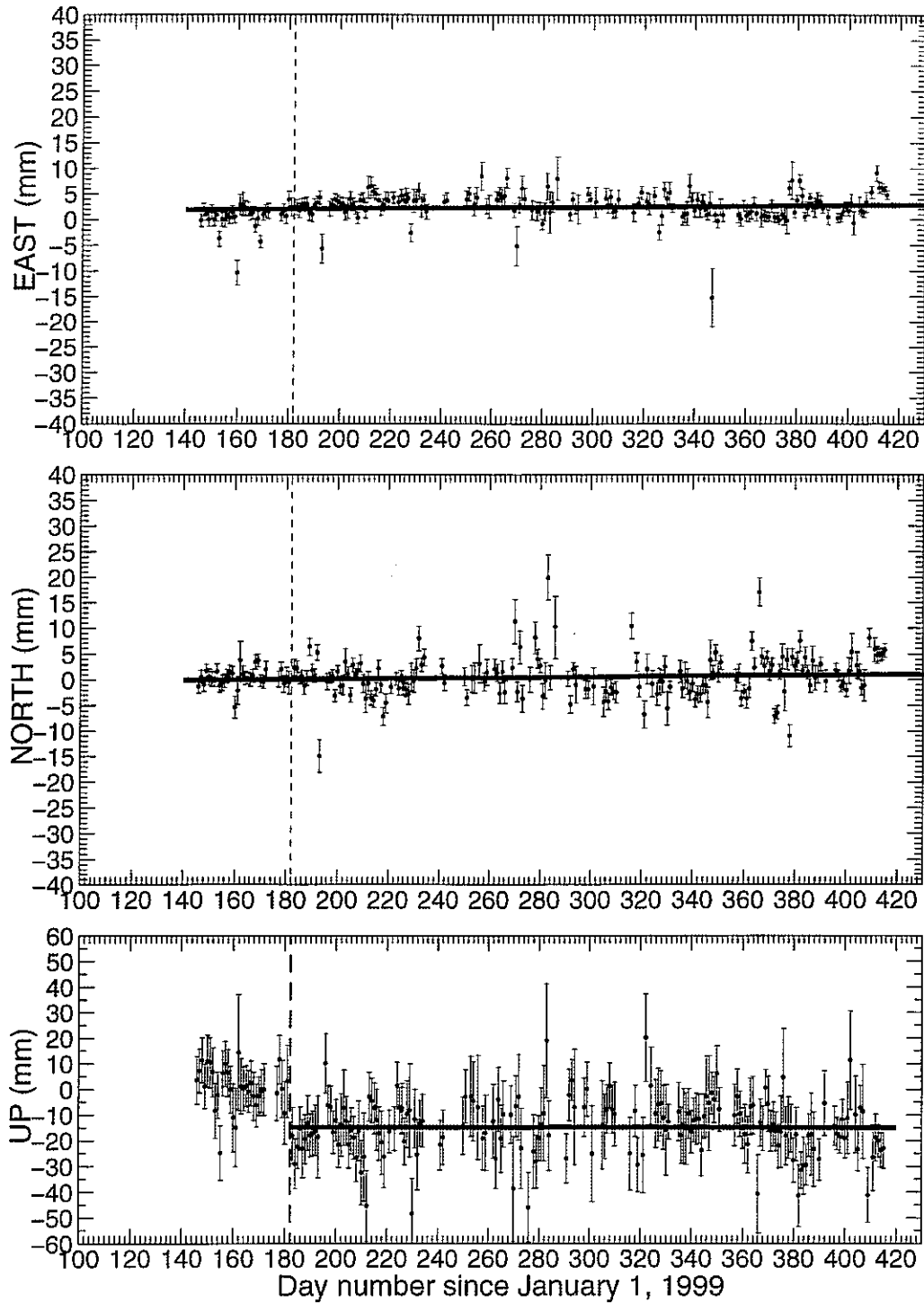
OLKE – REYK

Figure 11. *The horizontal and vertical motion of OLKE relative to REYK as a function of time, since the start of the measurements there. Each dot represents a 24 hour solution. The motion in east, north and up directions is defined to be positive, and is given in units of millimeters. The error bars indicate 1σ confidence limits. The thick black lines show the best fit (weighted least squares) velocities calculated for each component of motion, after outliers have been removed. The antenna radome was installed on day 182 (shown with dotted vertical black lines). The radome was re-oriented on day 209.*

21

5.2 The Mýrdalsjökull area

The time series from SOHO and HVOL are short and there are several data gaps due to power failures. The antenna tribrack was replaced on SOHO on day 313, 1999, causing an increase in antenna height of 1.3 mm. This antenna height change is included in the data analysis. SOHO and HVOL are the only stations in the network with antenna tribracks for leveling and centering the antennas.

5.2.1 SOHO

Figure 12 shows the relative motion of SOHO compared to REYK as a function of time. The average station coordinates for GPS week 1029 (September 26 – October 3, 1999) are used as a reference in the calculation. We find the best fit line through the data after removing 13 outliers (days 274, 289, 290, 315, 317, 320, 323, 325, 384, 387, 393, 403 and 408). The velocities we calculate for the station are 10 ± 4 mm/yr in east ($\chi^2_\nu = 1.2$) and 5 ± 6 mm/yr in north ($\chi^2_\nu = 2.6$). We find a subsidence rate of 5 ± 36 mm/yr ($\chi^2_\nu = 0.9$) after day 311. The time series before day 311 is to short to allow an estimate of the vertical velocity.

5.2.2 HVOL

Figure 13 shows the same as Figure 12 for HVOL. The average station coordinates for GPS week 1033 (October 24–31, 1999) are used as a reference in the calculation. We calculate the velocity of HVOL relative to REYK, after removing 11 outliers (days 292, 294, 300, 320, 325, 362, 365, 376, 393, 403 and 408). Assuming a constant velocity we find eastward motion of 3 ± 8 mm/yr ($\chi^2_\nu = 1.0$), northward of 5 ± 10 mm/yr ($\chi^2_\nu = 1.9$) and subsidence of 48 ± 30 mm/yr ($\chi^2_\nu = 0.6$). The antenna radome was installed at the same time as the antenna.
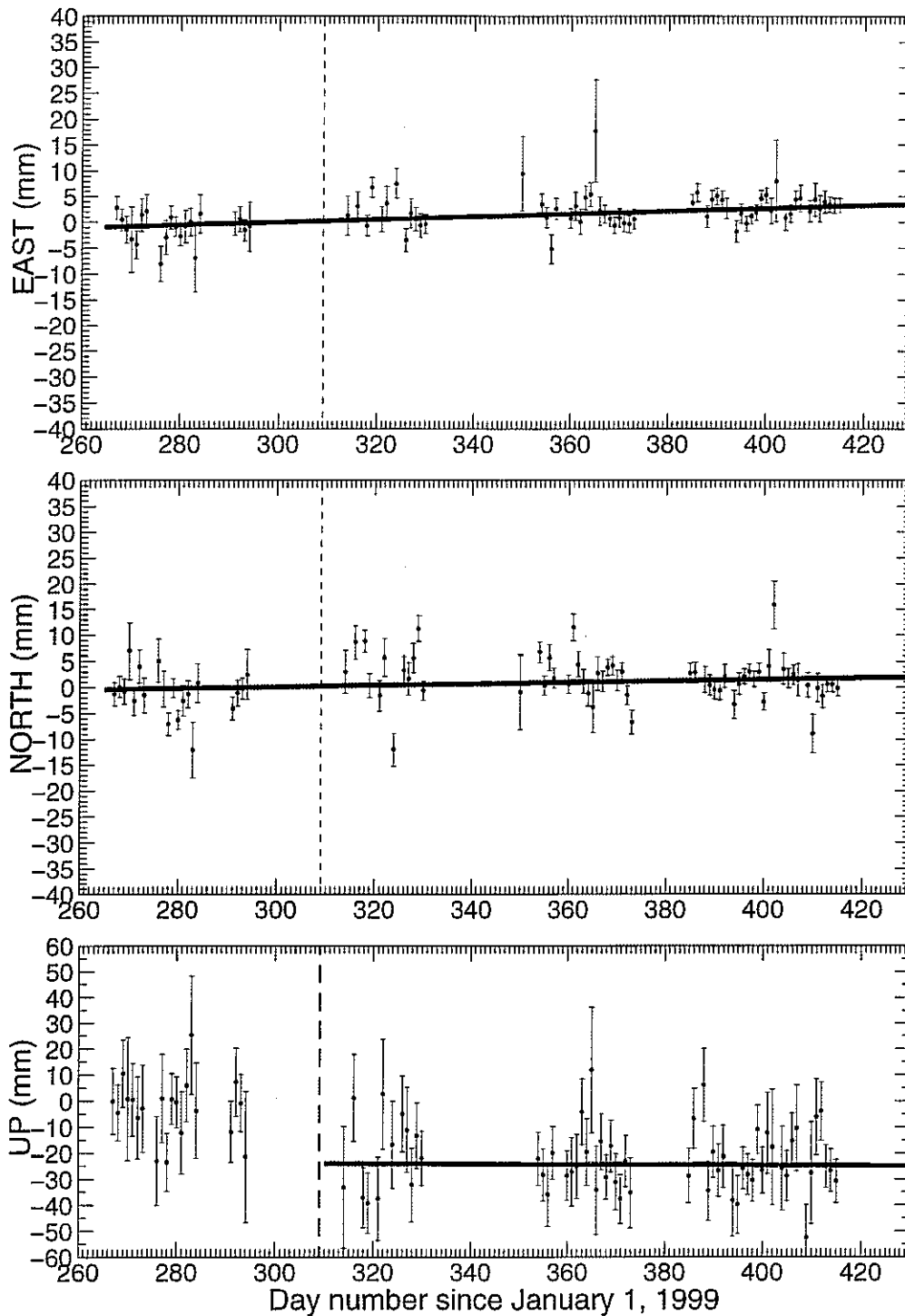
SOHO – REYK

Figure 12. *The horizontal and vertical motion of SOHO relative to REYK as a function of time, since the start of the measurements there. Each dot represents a 24 hour solution. The motion in east, north and up directions is defined to be positive, and is given in units of millimeters. The error bars indicate 1σ confidence limits. The thick black lines show the best fit (weighted least squares) velocities, calculated for each component of motion, after outliers have been removed. The antenna radome was installed on day 309 (shown with dotted vertical black lines). The tribrack was replaced on day 311. Note that the time scale is different from previous figures.*
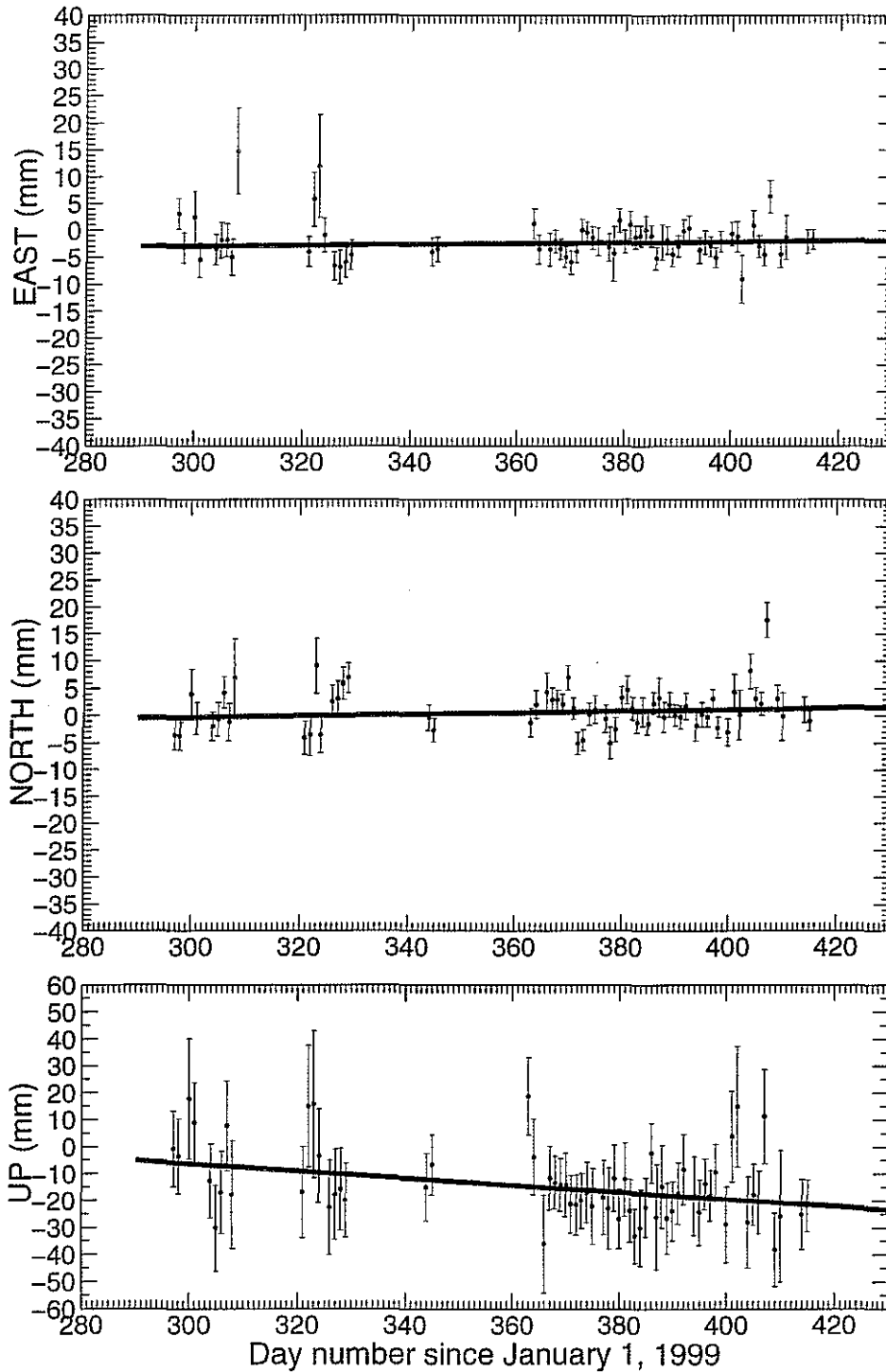
HVOL – REYK

Figure 13. *The horizontal and vertical motion of HVOL relative to REYK as a function of time, since the start of the measurements there. Each dot represents a 24 hour solution. The motion in east, north and up directions is defined to be positive, and is given in units of millimeters. The error bars indicate 1σ confidence limits. The thick black lines show the best fit (weighted least squares) velocities calculated for each component of motion, after outliers have been removed. The antenna radome was installed at the same time as the antenna. Note that the time scale is different from previous figures.*

24

6 ABSOLUTE STATION VELOCITIES

We have also processed the data from our network using the GIPSY/OASIS software (Webb and Zumberge 1993). While the Bernese software is based on parameter elimination using the double difference technique, GIPSY/OASIS processes undifferenced observation. Therefore, common parameters such as the clock parameters of the GPS satellites and receivers have to be estimated in GIPSY/OASIS, which are eliminated by the double difference technique used by the Bernese software. In principle, however, these two methods give the same results. GIPSY/OASIS offers one special processing strategy which is called *precise point positioning* (Zumberge et al. 1997). We use precise satellite clock and orbit information supplied by JPL, and do not estimate these parameters in our analysis. Precise point positioning is thus possible using data from only one station. The main advantage of this procedure is the reduction of computer time, since the system of normal equations is fairly small, because the size of the normal equation system grows as the square of the number of stations. The processing of data from a single station using the point positioning method, takes less than two minutes on a HP-UX K 360 workstation. A month of data from approximately 20 stations can therefore be processed in a few hours. Another advantage of the precise point positioning method is that it allows one to estimate absolute station coordinates in the ITRF97 reference system without using data from fiducial stations.

GPS data from 21 stations covering the margin of the North Atlantic and the permanent stations in Iceland were processed using GIPSY/OASIS. Instead of fixing ambiguities, only float solutions using the L_3 combination are computed, which are equivalent to fixed solutions when the observation window is longer than 8–12 hours (Mervart 1995). An elevation cut-off angle of $10°$ and the Niell mapping function (Niell 1993) were used for the estimation of tropospheric parameters. GIPSY/OASIS was also used to estimate absolute station velocities from the daily coordinate solutions, using the full covariance information. The variances of the individual solutions are underestimated in GIPSY. A more realistic estimation of the variance for the final coordinate and velocity estimation was obtained by scaling them by a factor of 2.7.

Figure 14 shows the east, north and up components of the absolute motion of REYK in the ITRF97 as a function of time. Outliers with large standard deviations or large offsets from the sample mean were removed. The largest component of motion of REYK is towards north. The estimated absolute velocities of the IGS stations in the ITRF97, and the 2σ errors are given in Table 3 and Figure 15. For comparison, Figure 15 also shows the expected station velocities calculated from the NNR-NUVEL-1A model (red arrows) (Argus and Gordon 1991). The agreement with the model is fairly good, except at the station pairs in Ny Alesund (NYAL/NYA1) and Reykjavík (REYK/REYZ). These locations have two antennas operated within a few meters of each other. The antennas in Reykjavík are about 1 m apart, and about 8 m in Ny Alesund. The differences in velocities are probably due to the short time series. Data from the station REYK were processed for the period between March 1999 and February 2000, whereas data for the station REYZ were only available after July 19, 1999. In general most velocities are statistically significant at the 2σ level.

The motion of the ISGPS stations relative to REYK are given in Table 4. The motion between REYK and REYZ is statistically significant even though both markers are mounted in the same concrete construction. Therefore, the velocities from these rather short time series do not seem to be entirely reliable. It is worthwhile to note that the 2σ errors in the estimates of relative motion (Table 4) are larger than for the absolute motion (Table 3). The reason is that there
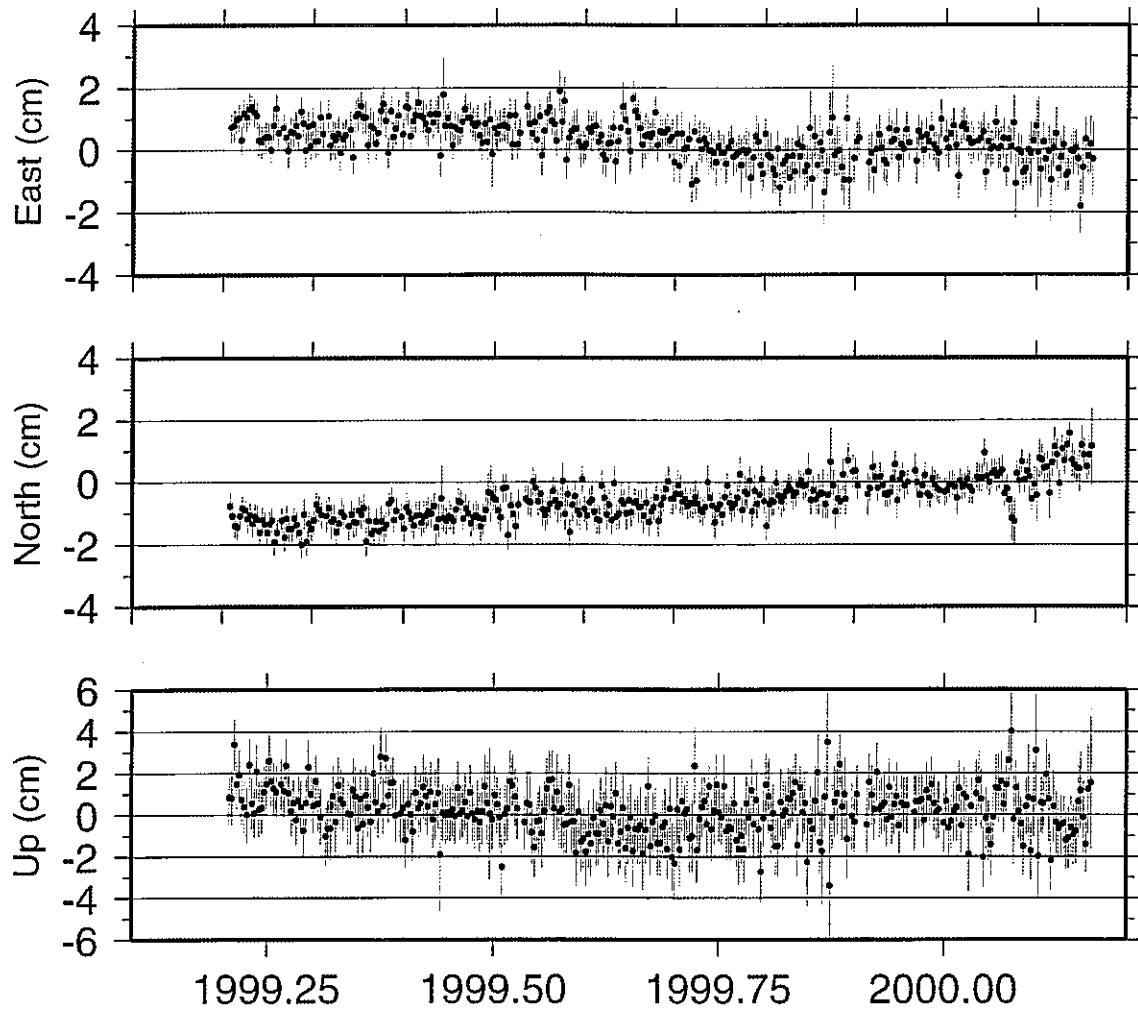
25

REYK

Figure 14. *Time series of the absolute motion of the station REYK in the ITRF97. Motion in the east, north and up directions is defined to be positive, and is presented in units of centimeters with 1σ error bars.*

Station	V_E (mm/yr)	V_N (mm/yr)	V_U (mm/yr)
ALGO	-15 ± 2	2 ± 1	-1 ± 5
HERS	16 ± 2	10 ± 2	-7 ± 5
KELY	-18 ± 4	11 ± 3	1 ± 8
KIRU	7 ± 3	18 ± 2	38 ± 7
KOSG	14 ± 2	16 ± 1	-1 ± 4
NYA1	6 ± 2	15 ± 2	7 ± 7
NYAL	12 ± 2	16 ± 2	16 ± 8
ONSA	13 ± 2	14 ± 1	0 ± 5
STJO	-11 ± 2	12 ± 1	-9 ± 4
THU1	-17 ± 2	-2 ± 2	-1 ± 7
WTZR	20 ± 2	14 ± 1	-2 ± 5
TROM	15 ± 3	15 ± 3	23 ± 9
HOFN	15 ± 3	9 ± 2	6 ± 7
REYK	-11 ± 2	19 ± 2	-8 ± 5
REYZ	-5 ± 5	25 ± 4	-2 ± 12

Table 3. *Absolute velocities in the ITRF97, using results from GIPSY analysis of data collected before March 1, 2000. The station velocities, V, are in east (E), north (N) and up (U). The reported uncertainty is at the 2σ level.*

Station	V_E (mm/yr)	V_N (mm/yr)	V_U (mm/yr)
HLID	1 ± 5	-11 ± 4	-27 ± 13
HVER	7 ± 3	-6 ± 2	-10 ± 7
HVOL	3 ± 15	13 ± 11	-29 ± 36
OLKE	2 ± 4	-1 ± 3	9 ± 9
SOHO	25 ± 8	3 ± 6	-36 ± 20
VOGS	13 ± 3	-4 ± 3	-13 ± 8
REYZ	6 ± 5	6 ± 4	6 ± 13

Table 4. *Calculated velocities using results from GIPSY analysis of data collected before March 1, 2000. The station velocities, V, are in east (E), north (N) and up (U), relative to REYK. The reported uncertainty is at the 2σ level. The velocities are calculated assuming a linear fit to each component of motion during the whole period. Effects due to radome installation are not considered.*
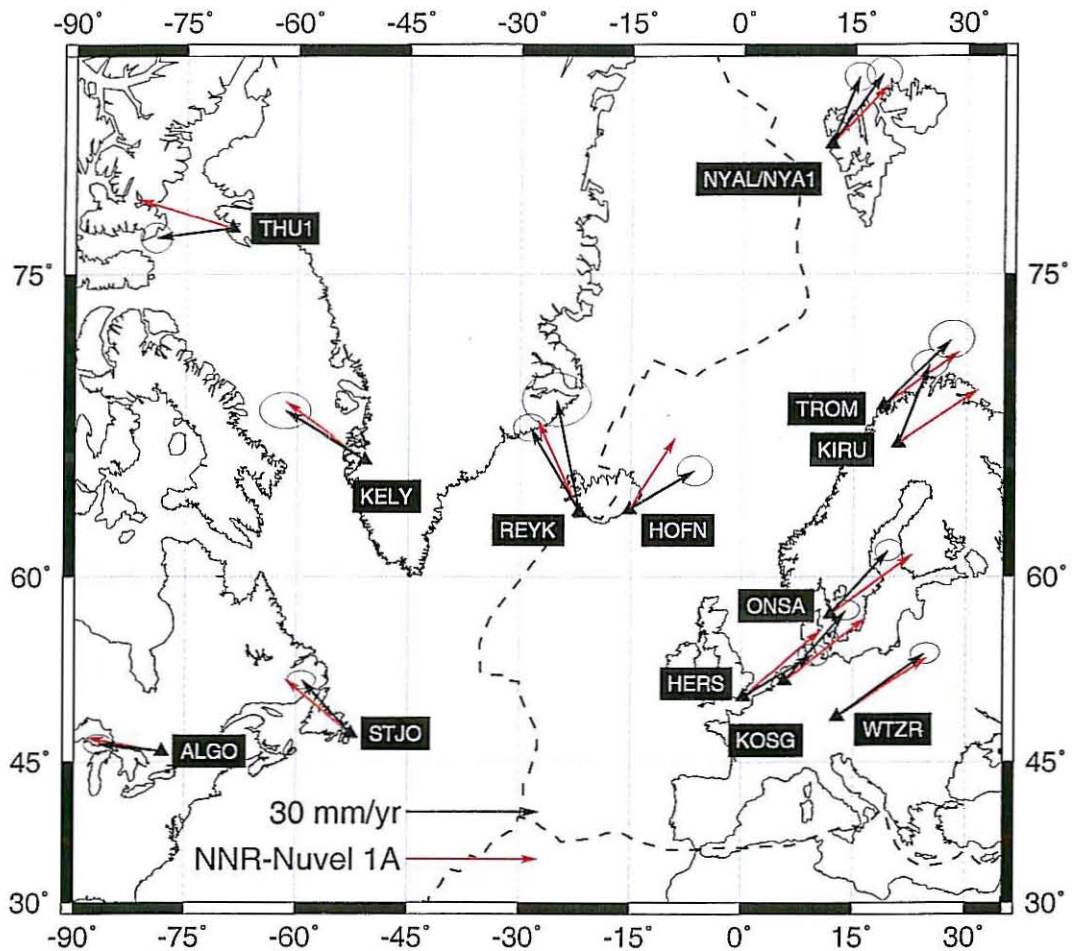
Figure 15. *Absolute horizontal motion in the ITRF97 for the IGS stations processed with GIPSY/OASIS (black arrows with error ellipses) and the corresponding NNR-NUVEL-1A velocities (red arrows) (Argus and Gordon 1991). The error ellipses show 2σ confidence limits.*

are no correlations between coordinates of different stations, since the stations are processed individually in the point positioning scheme. This, in turn, causes the errors of relative velocity estimations from the point positions to be larger than errors for the relative positioning (Table 2). Comparing Table 2 and Table 4, we see that the station velocities agree at the 2σ level, for all but a few components. Note that possible effects of radome installation were not considered when estimating the the vertical velocities in Table 4. Longer time series will provide more robust velocity estimates from both analysis methods and a better basis for comparison.

7 DISCUSSION

7.1 The Hengill area

Figure 16 shows the velocities of the stations in the Hengill area relative to REYK, estimated from the Bernese analysis. The horizontal velocities are shown with blue arrows. The error ellipses show the 2σ confidence limits. The vertical velocities are shown with green arrows, and the uncertainties with red bars. We see that all the stations in the Hengill area are moving east relative to REYK. The eastward velocity increases from OLKE to VOGS. The east and north components of velocity at VOGS translate to a motion of 12.2 ± 1 mm/yr in direction N99°E $\pm 5°$. The NUVEL-1A plate motion of the Eurasian plate relative to the North American plate is 18.5 mm/yr in direction N104°E for Vogsósar (shown with a purple arrow on Figure 16). The station VOGS appears to be moving at about 70% of the full NUVEL-1A plate velocity relative to REYK. The direction of motion agrees with the direction of relative plate motion of the Eurasian plate, assuming that the North American plate is fixed. This suggests that the signal observed at VOGS is primarily showing the relative plate motion between the North American and the Eurasian plates, and that VOGS is within the plate boundary zone, hence not moving at the full spreading rate.

The southward motion is largest at HVER (5 ± 1 mm/yr) but barely significant at the other stations. OLKE is closest to Hrómundartindur, and appears to be moving vertically at a rate of 0 ± 5 mm/yr, which is a considerably lower rate of deformation than estimated for the period 1993–1998. A longer uninterrupted time series is needed to more accurately determine the long-term vertical rate. An uplift rate of about 20 mm/yr is estimated for the Hrómundartindur area from various geodetic data from 1993 to 1998 (Sigmundsson et al. 1997; Feigl et al. 2000). GPS network measurements were done in the Hengill area in August and November 1998, and March 1999. The uplift at station RKOT, which is between OLKE and HVER, was significant during the period from August to November 1998, but not significant from November 1998 to March 1999 (Hreinsdóttir 1999). Network GPS measurements in the Hengill area done by the National Energy Authority (NEA) (Þorbergsson 1999) in June 1998 and June 1999, indicate uplift of almost 3 cm at the station closest to OLKE (7393), relative to station HH45, which is about 10 km NW of Ölkelduháls. We plan to re-analyze the data collected by the NEA using REYK as a reference, to determine if this uplift rate is influenced by motions of HH45.

A dimensionless number termed "strain release", calculated by 10^{5+M_L} (Böðvarsson et al. 1996), is useful to estimate seismic deformation. The seismic strain release for the Hengill area is about 6×10^{10} for the year 1998, and about 4×10^9 for 1999, using all earthquakes with M_L larger than 1.0. It is therefore clear that the seismic rate of deformation during 1998 is an order of magnitude larger than for 1999. It is possible that the large earthquake sequence of 1998 changed the dynamics of the system and we are entering a period of lower rates of deformation. A swarm of earthquakes occurred about 2–4 km east of Ölkelduháls on May 25, 1999
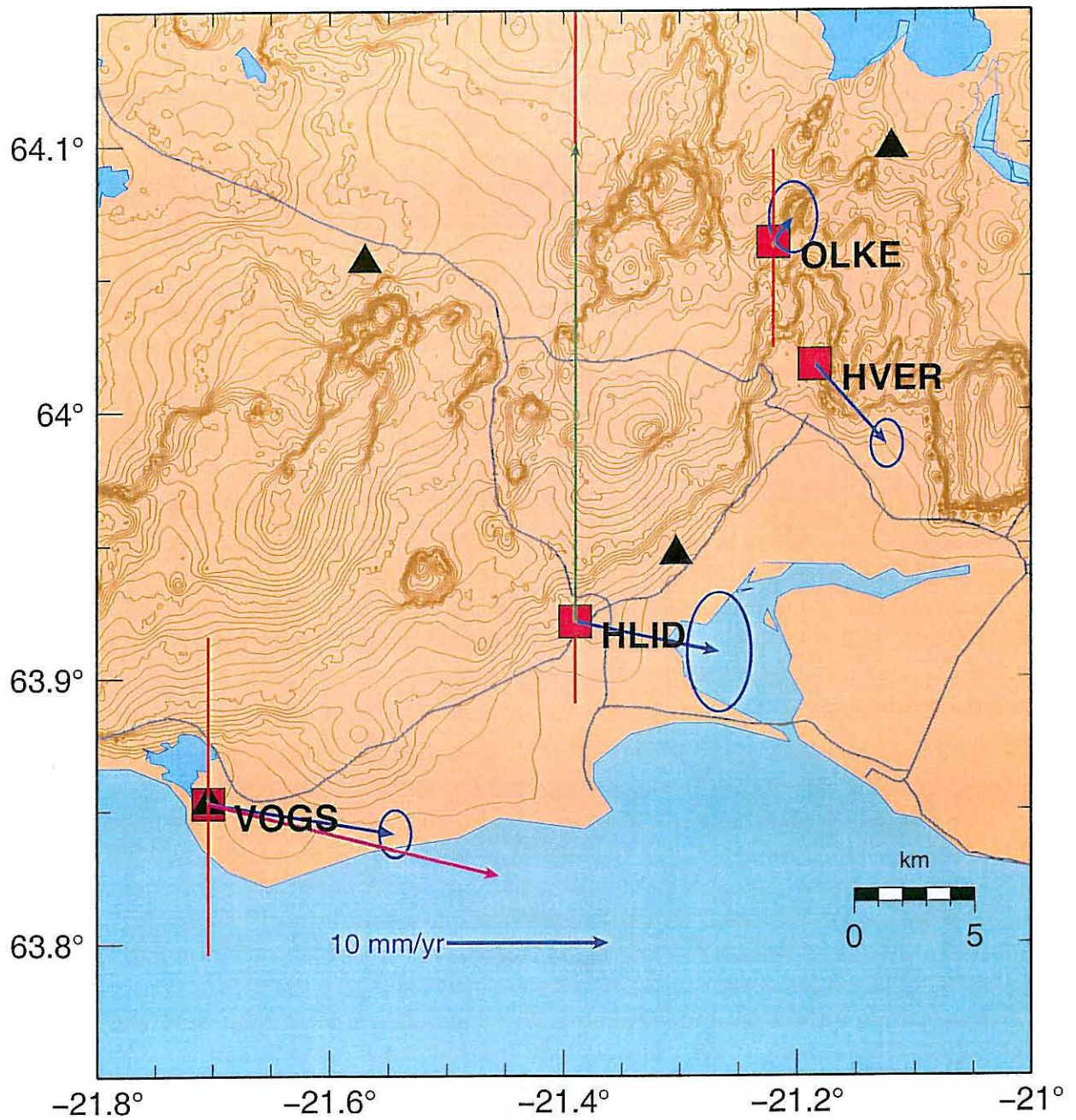
Figure 16. *Velocities of stations in the Hengill area relative to REYK. The horizontal velocities are shown with blue arrows and 2σ error ellipses. The vertical velocities are shown with green arrows, and the uncertainties with red bars. The vertical velocity at HVER was not estimated. The purple arrow at VOGS shows the estimated NUVEL-1A plate motion (18.5 mm/yr).*
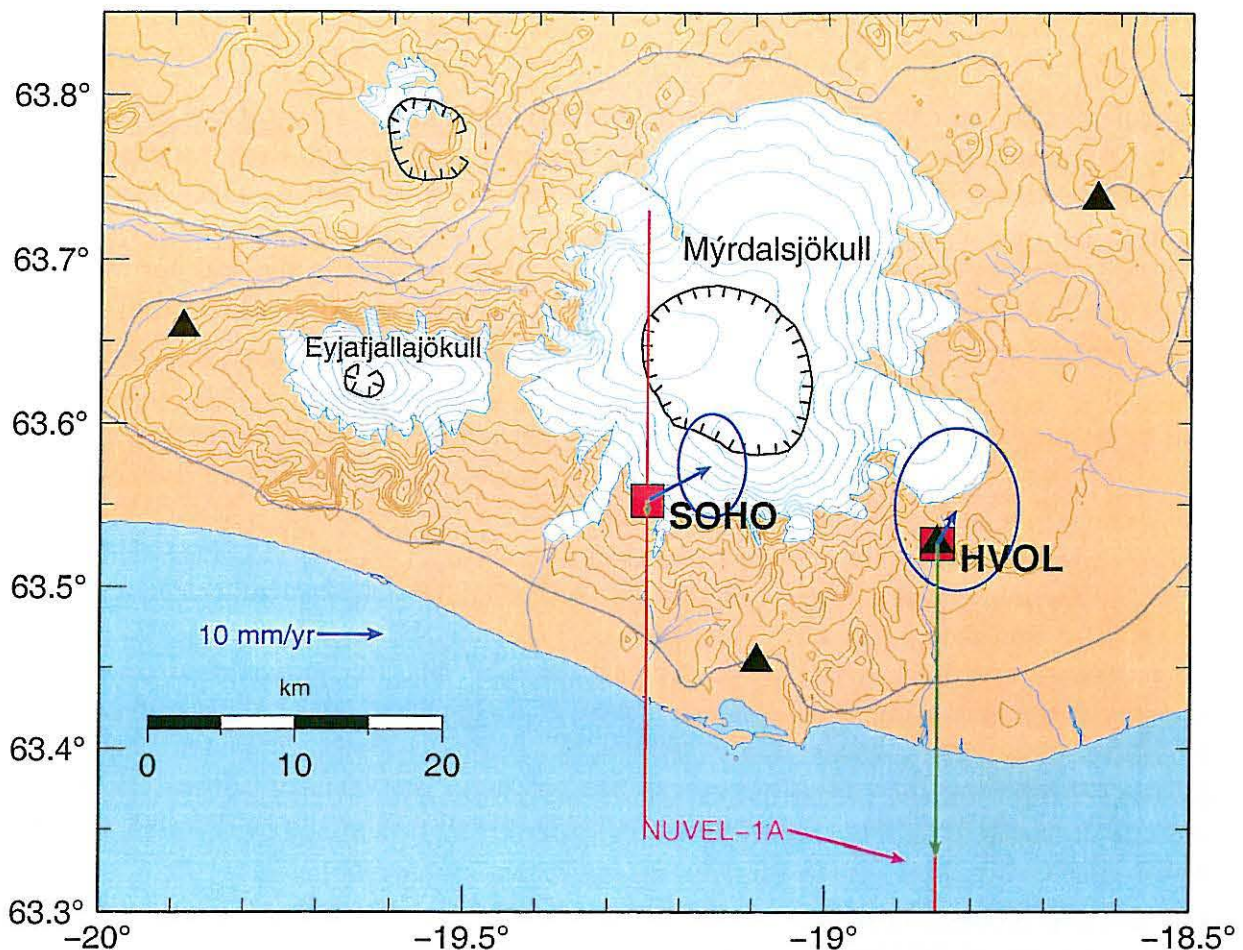
Figure 17. *Velocities of stations south of Mýrdalsjökull area relative to REYK. The horizontal velocities are shown with blue arrows and 2σ error ellipses. The vertical velocities are shown with green arrows, and the uncertainties with red bars. The purple arrow shows the calculated NUVEL-1A plate motion relative to REYK (18.6 mm/yr), assuming that the stations are on the Eurasian plate.*

(day 145), on the day that the station OLKE was installed. Four of the earthquakes recorded had M_L in the range of 3.0-3.9. It is possible that some aseismic motion continued in the area following the swarm, that might affect the rate of deformation at OLKE. In any case it is likely that the rates of deformation are highly variable, changing significantly over a period of a few months. Longer GPS time series are needed to test this hypothesis. Synthetic Radar Aperture (SAR) measurements in the Hengill area could provide independent information on the absolute vertical motion during 1999, although the resolution of temporal variation will not be as detailed as can be obtained with CGPS measurements.

7.2 The Mýrdalsjökull area

Figure 17 shows the velocities of the stations south of Mýrdalsjökull relative to REYK from the Bernese analysis. The horizontal velocities are shown with blue arrows and 2σ error ellipses. The vertical velocities are shown with green arrows, and the uncertainties with red bars. For comparison we show the calculated NUVEL-1A plate motion relative to REYK, which is 18.6 mm/yr (purple arrow), assuming that the stations are on the Eurasian plate. Longer time series are needed before we can determine what part of the signal at the stations is due to plate motions and what is caused by local volcanic sources. The time series at SOHO and HVOL are still short and there are many gaps in the data. As with the other stations, there are large uncertainties in the

vertical velocity estimates. It is therefore not yet clear whether the apparent rate of subsidence at HVOL is real, which could indicate that the magma system beneath Katla is deflating. The eastward motion of SOHO is the only component of motion that is (barely) significant at the 2σ level. HVOL does not show any significant horizontal motion during the time period we analyzed. This is in agreement with GPS network measurements in the area for the period August to November 1999 that show little motion at stations east of Eyjafjallajökull (Sturkell et al. 2000).

Theoretical models have been used to calculate surface deformation in the area around Katla and Eyjafjallajökull (Ágústsson 2000). An ellipsoidal source at the center of the Katla caldera (63.65°N, 19.10°W) with a centroid depth of 4 km and a volume increase of 0.1 km³ would cause about 5 cm in eastward, 8 cm in southward and 3 cm upward motion at SOHO. The station at HVOL would detect 4 cm westward, 4 cm southward and 1 cm of uplift, for the same source model. If the source was centered at 4 km depth beneath the Eyjafjallajökull caldera (63.63°N, 19.63°W) it would cause an eastward motion of 4 cm at SOHO and 1 cm at HVOL, about 2 cm southward motion at SOHO, and less than 1 cm at HVOL. The vertical motion would not be significant at these stations. A spherical source at 7.5 km depth, under either caldera, would produce slightly larger signals at both stations (K. Ágústsson, pers. communication, 2000). Little is known about dike intrusions under these volcanoes, and therefore difficult to estimate reasonable source parameters for such events and how well they would be detected at SOHO and HVOL.

The inherent problem in monitoring crustal deformation due to magma movements beneath Katla and/or Eyjafjallajökull is that the volcanoes are covered by glaciers, and the closest stations are far away from the caldera centers, where the largest deformation is expected. It is therefore possible that magma accumulation of up to 0.1 km³ could occur at shallow depth beneath Katla or Eyjafjallajökull without being detected at SOHO and/or HVOL.

8 CONCLUSIONS

This report discusses the first results of the continuous GPS network (ISGPS) in Iceland. The first station was installed in mid-March 1999, and we analyze the data up to February 20, 2000. We estimate station velocities relative to the CGPS station in Reykjavík (REYK), by fitting a straight line to each component of motion.

The main conclusions can be summarized as:

- Station VOGS appears to be moving at about 70% of the NUVEL-1A plate velocity, relative to REYK.

- Very little motion is observed at station OLKE, indicating that the large rates of deformation observed near Hrómundartindur from 1993 to mid-1998, have decreased since mid-1999.

- The short time series and large noise in the vertical component cause the velocity estimates to be quite uncertain, particularly for the vertical component.

- We detect large vertical offsets (about 21–22 mm) due to radome installation.

- Insignificant motion is detected at SOHO and HVOL, indicating that magma accumulation at shallow depth beneath Katla during the observation period is less than 0.1 km³.

32

Future plans include:

- Install two new CGPS stations near Eyjafjallajökull to improve monitoring of deformation due to possible magma movements or accumulation beneath the volcano.

- Determine the effects of radome installation in our network.

- Use predicted orbits in our analysis for near real-time data processing.

- Improve network solutions and velocity estimates with longer time series and more sophisticated software.

9 ACKNOWLEDGEMENTS

10   REFERENCES

Argus, D.F. and R.G. Gordon 1991. No-net-rotation model of current plate velocities incorporating plate motion model NUVEL-1. *Geophys. Res. Lett.* 18, 2038–2042.

Ágústsson, K. 1998. Earthquake swarm on Hellisheiði and Hengill in May–July 1998 (Jarðskjálftahrina á Hellisheiði og í Hengli í maí-júlí 1998). *Greinargerð Veðurstofu Íslands* VÍ-G98040-JA06. Report, Icelandic Meteorological Office, Reykjavík (in Icelandic).

Ágústsson, K. 2000. Katla and Eyjafjallajökull – a few models and thoughts (Katla og Eyjafjallajökull – nokkur líkön og hugleiðingar). *Greinargerð Veðurstofu Íslands* VÍ-G00002-JA01. Report, Icelandic Meteorological Office, Reykjavík (in Icelandic).

Árnadóttir, Þ., S.Th. Rögnvaldsson, K. Ágústsson, R. Stefánsson, S. Hreinsdóttir, K.S. Vogfjörð and G. Þorbergsson 1999. Seismic swarms and surface deformation in the Hengill area, SW Iceland. *Seismol. Res. Lett.* 70, 269.

Boucher, C., Z. Altamimi and P. Sillard 1999. The 1997 International Terrestrial Reference Frame (ITRF97). *IERS Technical Note* 27. Observatoire de Paris, France.

Böðvarsson, R., S.Th. Rögnvaldsson, S.S. Jakobsdóttir, R. Slunga and R. Stefánsson 1996. The SIL data acquisition and monitoring system. *Seismol. Res. Lett.* 67, 35–46.

Böðvarsson, R., S.Th. Rögnvaldsson, R. Slunga and E. Kjartansson 1999. The SIL data acquisition system — at present and beyond year 2000. *Phys. Earth Planet. Inter.* 113, 89–101.

Camitz, J., F. Sigmundsson, G. Foulger, C.-H. Jahn, C. Völksen and P. Einarsson 1995. Plate boundary deformation and continuing deflation of the Askja volcano, North Iceland, determined with GPS, 1987–1993. *Bull. Volcanol.* 57, 136–145.

DeMets, C., R.G. Gordon, D.F. Argus and S. Stein 1990. Current plate motions. *Geophys. J. Int.* 101, 425–478.

DeMets, C., R.G. Gordon, D.F. Argus and S. Stein 1994. Effect of recent revisions to the geomagnetic reversal time scale on estimates of current plate motions. *Geophys. Res. Lett.* 21, 2191–2194.

Dixon, T.H., A. Mao, M. Bursik, M. Heflin, J. Langbein, R. Stein and F. Webb 1997. Continuous monitoring of surface deformation at Long Valley caldera, California, with GPS. *J. Geophys. Res.* 102, 12017–12034.

Einarsson, P. 2000. Events related to a flood in Jökulsá á Sólheimasandi in July 1999 (Atburðarás í tengslum við hlaup í Jökulsá á Sólheimasandi í júlí 1999). In: Abstracts from the February meeting of the Geoscience Society of Iceland, Reykjavík, February 17, 2000 (in Icelandic).

Einarsson, P. and K. Sæmundsson 1987. Earthquake epicenters 1982–1985 and volcanic systems in Iceland. In: Þorsteinn I. Sigfússon (editor), *Í hlutarins eðli*. Map accompanying festschrift for Þorbjörn Sigurgeirsson. Menningarsjóður, Reykjavík.

Erlendsson, P. 1996. *Mapping of earthquake fractures east of Brennisteinsfjöll* (Kortlagning jarðskjálftasprungna austan Brennisteinsfjalla). B.S. thesis, University of Iceland, Reykjavík (in Icelandic).

Estey, L. and C. Meertens 1999. TEQC: The multipurpose toolkit for GPS/GLONASS data. *GPS Solutions* 3, 44–49.

EUREF 2000. The permanent European Reference Frame (EUREF) network. URL: http://homepage.oma.be/euref/eurefhome.html. Last modified April 19.

Feigl, K.L., J. Gasperi, F. Sigmundsson and A. Rigo 2000. Crustal deformation near Hengill volcano, Iceland, 1993–1998: coupling between magmatic activity and faulting inferred from elastic modeling of satellite radar interferograms. *J. Geophys. Res.*, submitted.

Foulger, G. 1987. A GPS geodetic survey of the northern volcanic zone of Iceland 1987. *EOS, Trans. Am. Geophys. Un.* 68, 1236.

Foulger, G., R. Bilham, W.J. Morgan and P. Einarsson 1987. The Iceland GPS geodetic field campaign 1986. *EOS, Trans. Am. Geophys. Un.* 68, 1809.

Gurtner, W. 1994. RINEX: the Receiver-Independent Exchange Format. *GPS World*, July, 48–52.

Hackman, M.C., G.C.P. King and R. Bilham 1990. The mechanism of the South Iceland seismic zone. *J. Geophys. Res.* 95, 339–351.

Hamburger, M., C. Meertens, S. Owen, T. Dixon and S. Stein 1999. Meeting report: UNAVCO volcano geodesy workshop. URL: http://www.unavco.ucar.edu/science_tech/volcano/-meetings/sep_99.html. Last modified October 23.

Heki, K., G. Foulger, B. Julian and C.-H. Jahn 1993. Plate dynamics near divergent plate boundaries: Geophysical implications of post-rifting crustal deformation in NE Iceland. *J. Geophys. Res.* 98, 14279–14297.

Hreinsdóttir, S. 1999. *GPS geodetic measurements on the Reykjanes Peninsula, SW Iceland: crustal deformation from 1993 to 1998.* M.S. thesis, University of Iceland, Reykjavík.

Hreinsdóttir, S., P. Einarsson and F. Sigmundsson 2000. Crustal deformation at the oblique spreading Reykjanes peninsula, SW Iceland: GPS measurements from 1993 to 1998. *J. Geophys. Res.*, submitted.

Jahn, C.-H. 1990. A highly precise GPS-epoch measurement in the northeast volcanic zone of Iceland. In: J.P. Paquet, J. Flick and B. Ducarme (editors), *Cahiers du Centre Européen de Géodynamique et de Sismologie.* Luxembourg, 292–304.

Leick, A. 1990. *GPS satellite surveying.* John Wiley & Sons, New York.

Linde, A.T., K. Ágústsson, I.S. Sacks and R. Stefánsson 1993. Mechanism of the 1991 eruption of Hekla from continuous borehole strain monitoring. *Nature* 365, 737–740.

Lisowski, M., S. Owen and P. Segall 1996. The Kiluea Volcano Hawaii, continuous GPS network: recent results. *EOS, Trans. Am. Geophys. Un.* 77, 808.

Mervart, L. 1995. Ambiguity resolution technique in geodetic and geodynamic applications of the Global Positioning System. Ph.D. thesis. *Geodätisch-geophysikalische Arbeiten in der Schweiz*, report nr. 53.

Niell, A. 1993. A new approach for the hydrostatic mapping function. In: *Proceedings of the International Workshop for Reference Frame Establishment and Technical Development in Space Geodesy.* Tokyo, Japan.

Rothacher, M. and L. Mervart 1996. *Bernese GPS software version 4.0.* Astronomical Institute, University of Berne, Berne, Switzerland.

Rögnvaldsson, S.Th., K. Ágústsson, B.H. Bergsson and G. Björnsson 1998a. Seismic network near Reykjavík – network discription and first results (Jarðskjálftamælanet í nágrenni Reykjavíkur – lýsing á mælaneti og fyrstu niðurstöður). *Rit Veðurstofu Íslands* VÍ-R98001-JA01. Research report, Icelandic Meteorological Office, Reykjavík.

Rögnvaldsson, S.Th., Þ. Árnadóttir, K. Ágústsson, Þ. Skaftadóttir, G.B. Guðmundsson, G. Björnsson, K.S. Vogfjörð, R. Stefánsson, R. Böðvarsson, R. Slunga, S.S. Jakobs-

dóttir, B. Þorbjarnardóttir, P. Erlendsson, B.H. Bergsson, S. Ragnarsson, P. Halldórsson, B. Þorkelsson and M. Ásgeirsdóttir 1998b. An earthquake swarm in Ölfus in November 1998 (Skjálftahrina í Ölfusi í nóvember 1998). *Greinargerð Veðurstofu Íslands* VÍ-G98046-JA09. Report, Icelandic Meteorological Office, Reykjavík (in Icelandic).

SCIGN 1999. SCIGN radome project. URL: http://www-socal.wr.usgs.gov/scign/group/dome. Last modified March 31.

Sigmundsson, F., P. Einarsson and R. Bilham 1993. Magma chamber deflation recorded by the Global Positioning System: the Hekla 1991 eruption. *Geophys. Res. Lett.* 19, 1483–1486.

Sigmundsson, F., P. Einarsson, R. Bilham and E. Sturkell 1995. Rift–transform kinematics in South Iceland: deformation from Global Positioning System measurements, 1986 to 1992. *J. Geophys. Res.* 100, 6235–6248.

Sigmundsson, F., P. Einarsson, S.Th. Rögnvaldsson, G. Foulger, K. Hodkinson and G. Þorbergsson 1997. 1994–1995 seismicity and deformation at the Hengill triple junction, Iceland: triggering of earthquakes by an inflating magma chamber in a zone of horizontal shear stress. *J. Geophys. Res.* 102, 15151–15161.

Stefánsson, R., R. Böðvarsson, R. Slunga, P. Einarsson, S.S. Jakobsdóttir, H. Bungum, S. Gregersen, J. Havskov, J. Hjelme and H. Korhonen 1993. Earthquake prediction research in the South Iceland seismic zone and the SIL project. *Bull. Seism. Soc. Am.* 83, 696–716.

Sturkell, E., F. Sigmundsson and P. Einarsson 1994. Strain accumulation 1986–1992 across the Reykjanes peninsula plate boundary, Iceland, determined from GPS measurements. *Geophys. Res. Lett.* 21, 125–128.

Sturkell, E., P. Einarsson and F. Sigmundsson 2000. Crustal deformation around Mýrdalsjökull and Eyjafjallajökull, 1967–2000. In: Abstracts from the February meeting of the Geoscience Society of Iceland, Reykjavík, February 17, 2000.

Sæmundsson, K. 1995. Hengill, geological map (bedrock) 1:50000.

UNAVCO 1999. Data management software. URL: http://www.unavco.ucar.edu/software. Last modified December 27.

Webb, F.H. and J.F. Zumberge 1993. An introduction to GIPSY/OASIS-II precision software for the analysis of data from the Global Positioning System. *JPL Publications* No. D-11088. Jet Propulsion Laboratory, Pasadena, California.

Webb, F., M. Bursik, T.H. Dixon, F. Farina, G. Marshall and R. Stein 1995. Inflation of Long Valley caldera, California, from one year of continuous GPS observations. *Geophys. Res. Lett.* 22, 195–198.

Wessel, P. and W.H.F. Smith 1991. Free software helps map and display data. *EOS, Trans. Am. Geophys. Un.* 72, 441 and 445–446.

Zumberge, J.F., M.B. Heflin, D.C. Jefferson, M.M. Watkins and F. Webb 1997. Precise point positioning for the efficient and robust analysis of GPS data from large networks. *J. Geophys. Res.* 102, 5005–5017.

Þorbergsson, G. 1999. Nesjavallaveita. GPS measurements and measurements of cracks in the Hengill area 1999 (Nesjavallaveita. GPS-mælingar og mælingar yfir sprungur á Hengilssvæði 1999). *Skýrsla Orkustofnunar* OS-99077. Technical Report, National Energy Authority, Reykjavík (in Icelandic).

Kápumynd: Klósigar (vatnsklær)
Ljósm.: Guðmundur Hafsteinsson, veðurfræðingur